

Mechanisms underlying American marten (*Martes americana*) winter rest site selection  
across the Western Great Lakes Region

A THESIS  
SUBMITTED TO THE FACULTY OF THE  
UNIVERSITY OF MINNESOTA  
BY

Taylor Beau Velander

IN PARTIAL FULFILLMENT OF THE REQUIREMENTS  
FOR THE DEGREE OF  
MASTER OF SCIENCE

Dr. Ron Moen, Co-Adviser  
Dr. Michael Joyce, Co-Adviser

July 2022



## **Acknowledgments**

I thank my advisors, Ron A. Moen and Michael J. Joyce, for their dedication toward helping me with my education and research. Thank you to Guy Sander for the knowledge and guidance he has provided. We thank our collaborators Robert Sanders and Angela Kujawa from the Little River Band of Ottawa Indians, and Paul Keenlance from Grand Valley State University, for their assistance on this project. We appreciate Michael McMahon for his help with data collection.

I am grateful for the University of Minnesota Duluth, Department of Biology for giving me teaching assistantships, the Natural Resources Research Institute for financial and logistical support, and the Integrated Biosciences Graduate Program and its faculty for additional support.

This project was funded by the Minnesota Environmental and Natural Resources Trust Fund as recommended by the Legislative-Citizen Commission on Minnesota's Resources (M.L. 2019, First Special Session, Chp. 4, Art. 2, Sec. 2, Subd. 03i. Den boxes for fishers and other cavity-nesting wildlife) and by the Great Lakes Restoration Initiative administered by the Bureau of Indian Affairs.

## Table of Contents

List of tables.....	iii
List of figures.....	iv
Chapter 1: A dynamic thermal model for predicting internal temperature of tree cavities and nest boxes.....	1
Overview.....	2
Introduction.....	2
Methods.....	7
Results.....	19
Discussion.....	24
Conclusion.....	30
Chapter 2: The role of ambient temperature and snowpack characteristics on American marten winter rest site selection in the Western Great Lakes Region.....	46
Overview.....	47
Introduction.....	47
Methods.....	53
Results.....	60
Discussion.....	66
Conclusion.....	73
Bibliography.....	83
Appendix.....	95

## List of tables

Table 1.1. Density, specific heat, and thermal conductivity values used for estimating model parameters.....	32
Table 1.2. Summary of thermal and physical characteristics of sampled natural cavities in the Superior and Chippewa National Forest, MN, USA.....	33
Table 1.3. Summary of thermal and physical characteristics of sampled natural cavities in the Manistee National Forest, MI, USA.....	35
Table 1.4. Summary of thermal and physical characteristics, and design of artificial cavity types used for model validation.....	37
Table 1.5. Summary statistics for natural cavities sampled in the Superior National Forest and Chippewa National Forest in Minnesota, USA.....	39
Table 1.6. Summary statistics for natural cavities sampled in the Manistee National Forest in Michigan, USA.....	40
Table 1.7. Summary statistics for artificial cavities sampled.....	41
Table 1.8. Summary of daily root mean squared error (RMSE) for artificial cavity types tested.....	43
Table 2.1. Summary of tree cavity characteristics in the Superior National Forest, MN USA, and the Manistee National Forest, MI USA.....	78

## List of figures

Figure 1.1. Schematic of the primary heat and mass transfers processes in a tree cavity system.....	31
Figure 1.2. Model results in natural and artificial cavities.....	38
Figure 1.3. Cumulative frequency distribution of daily root mean squared error (RMSE) for natural and artificial cavities.....	44
Figure 1.4. Examples of thermal arrest periods at 0°C.....	45
Figure 2.1. Winter ambient temperature in the Superior National Forest, MN USA, and the Manistee National Forest, MI USA.....	74
Figure 2.2 Winter snow depth in the Superior National Forest, MN USA, and the Manistee National Forest, MI USA.....	75
Figure 2.3. Daily snow depth, snow density, ambient temperature, and microhabitat temperature.....	76
Figure 2.4. Winter temperatures in tree cavities and subnivean sites in the Superior National Forest, MN USA, and Manistee National Forest, MI USA.....	77
Figure 2.5. Energetic cost of resting in tree cavities and subnivean sites during the winter in the Superior National Forest, Minnesota USA, and in the Manistee National Forest, Michigan USA.....	79
Figure 2.6. Relationship between energetic cost of thermoregulation and ambient temperature in tree cavities and subnivean microhabitats.....	80
Figure 2.7. Relationship between snow depth and average energy lost while inactive for one hour a day in subnivean microsites.....	81
Figure 2.8. Modified decision tree for selecting subnivean and tree cavity microsites.....	82

Chapter 1: A dynamic thermal model for predicting internal temperature of tree cavities  
and nest boxes

## Overview

Tree cavities are important microhabitats that many mammal species use as a secure place for resting and raising young. Cavities buffer ambient weather and moderate temperatures, which helps reduce the energetic costs of thermoregulation. The buffering capacity of tree cavities, however, varies with tree and cavity characteristics, making it difficult to estimate cavity-specific temperatures without the use of temperature loggers. Here, we introduce a dynamic model that incorporates fundamental processes of heat and mass transfer to predict the internal temperature of tree cavities as a function of cavity-specific physical characteristics and ambient temperature. To validate the model, we compared measured and modeled internal temperatures of 43 natural tree cavities used by American martens (*Martes americana*) or fishers (*Pekania pennanti*) and 27 artificial cavities designed for fishers. Cavities varied in physical and thermal characteristics, allowing us to assess the generalizability of the model. Predicted internal temperatures of natural and artificial cavities were similar to measured temperatures, with average RMSE values less than 1.77°C. Our results demonstrate that the model can accurately predict temperature within the tree cavities over time, has a tractable complexity that captures the main processes driving temperature within the tree cavity, is easily parameterized so it can be applied to many ecological questions, and is adaptable enough to be used in a range of conditions.

## Introduction

Many mammal and bird species use tree cavities for resting and raising young (Grüebler et al., 2014; Isaac et al., 2008; Maziarz et al., 2017; McComb and Noble,

1981b; Moore, 1945). Tree cavities provide protection from predators and favorable microclimates to inhabitants. Energetic costs of thermoregulation during periods of extreme ambient temperatures are reduced when birds and mammals use tree cavities (Du Plessis et al., 1994; Joyce, 2013; Kendeigh, 1961; Matthews et al., 2019; Sedgeley, 2001; Zalewski, 1997a). Further, favorable thermal conditions in tree cavities may reduce the energetic costs of reproduction, enhance egg viability, and increase offspring growth rate (Ardia et al., 2006; Clement and Castleberry, 2013; Wiebe and Swift, 2001).

Temperatures within tree cavities and other microhabitats are influenced by local weather conditions, site characteristics, and the thermal and structural properties of the microhabitat that modulate heat and mass transfer processes between the microhabitat and its environment (Kearney and Porter, 2017). For example, trees can partially block solar insolation and decrease local ambient temperatures (Berry et al., 2013; De Frenne et al., 2019; Leuzinger et al., 2010). Other site characteristics such as slope and aspect at the tree cavity site also affect temperature (Méndez-Toribio et al., 2016; Suggitt et al., 2011). Characteristics of the cavity, such as orientation of entrance holes, size of entrance holes, chamber volume, chamber diameter, wall thickness, internal surface area, and the specific heat capacity of the wood surrounding the cavity affect internal cavity temperatures (Ardia et al., 2006; Clement and Castleberry, 2013; MacLean, 1941; Paclík and Weidinger, 2007; Radmanović et al., 2014; Sedgeley, 2001). For example, temperatures are more stable, or have smaller temperature fluctuations throughout the day, in cavities located in large diameter trees (Coombs et al., 2010). This is, in part, because increased wood around cavity chambers resists heat flow between the cavity and the external environment. Similarly, temperatures in cavities with many entrance holes, or cavities

with large entrance holes, are likely less stable due to greater air movement into and out of the cavity.

Moisture also plays an important role in microhabitat temperature when water freezes and thaws. In trees without cavities, for example, wood temperature is partially governed by phase changes of water or sap that occur when temperatures reach freeze-thaw (Charrier et al., 2017; Derby and Gates, 1966; Graf et al., 2015; Reid et al., 2020; Zhao et al., 2021). Freeze-thaw is the temperature at which ice begins to melt or a liquid begins to freeze. Freeze-thaw for pure water is 0°C, but freeze-thaw can be slightly warmer or cooler for aqueous solutions such as tree sap (Derby and Gates, 1966; Graf et al., 2015; Reid et al., 2020; Zhao et al., 2021). Graf et al. (2015) describe the fundamental phase change dynamics within trees. Water frozen in a tree undergoes a phase change from a solid to a liquid state as temperatures in the tree reach freeze-thaw. During this phase change, the latent heat of fusion of ice keeps the wood at temperatures around freeze-thaw even if ambient temperatures climb above freeze-thaw temperatures. This period of relatively constant temperature around freeze-thaw is called a thermal arrest period, and it does not end until the ice fully thaws. An analogous scenario occurs during freezing, where the latent heat of solidification of liquid water creates a thermal arrest period around freeze-thaw until the water has fully solidified. Latent heat of water is also responsible for thermal arrest periods that occur during the freezing and thawing of moist soil (Kudriavtcev et al., 2016; Zhang et al., 2020; Zhou et al., 2018). In addition, phase change of water is also a key component of the development of the subnivean microhabitats, and is a process that allows the subnivium to maintain a temperature of around 0°C throughout the winter in areas with relatively deep snowpack (Cohen, 1994;

Kearney, 2020; Thompson et al., 2018). Temperatures in tree cavities should also be affected by phase changes of water in the tree cavity or in the cavity walls.

Many animals select cavities based in part on the relative thermal benefit they provide. Female fishers (*Pekania pennanti*), for example, select warm cavities early in the kit-rearing season to protect kits from cold temperatures, but select cooler cavities later in the denning season to prevent the kits from overheating (Matthews et al., 2019). Tree swallows (*Tachycineta bicolor*) prefer warmer artificial boxes early in the breeding season, suggesting that differences in temperatures between cavities can affect reproductive success (Ardia et al. 2006). Bats decrease the energetic costs of thermoregulation and promote fetal and juvenile growth by selecting cavities that are cooler during the day and warmer at night (Lausen and Barclay, 2003; Ruczyński, 2006). Bats also benefit from energy conservation strategies such as torpor and passive re-warming by selecting roost sites with different thermal characteristics (Lausen and Barclay, 2003).

Having the ability to estimate the temperature in tree cavities could improve our mechanistic understanding of the role of cavity characteristics on animal selection and ecology and provide a biological basis for management decisions. Temperature loggers are often used to make a direct connection between animal response and microhabitat temperature (Coombs et al., 2010; Fawcett et al., 2019; Isaac et al., 2008; Maziarz et al., 2017; Mersten-Katz et al., 2012; Paclík and Weidinger, 2007; Vonhof and Barclay, 1997; Wiebe, 2001). Temperature loggers, however, cannot predict historical tree cavity temperatures, and are limited to measuring temperatures in a single tree cavity and how long they can measure temperatures for. Alternatively, models can be used to predict

historical and future temperatures in multiple cavities as a function of changes in weather conditions, habitat characteristics, and cavity characteristics.

A variety of thermal modeling methods have been used to measure or estimate heat flow and temperatures of systems like tree cavities. Complex theoretical heat transfer equations can be used to model a broad range of heat and mass transfer processes (Kearney and Porter, 2017; Potter and Andresen, 2002; Reid et al., 2020; Westermann et al., 2013). This modeling approach often requires many parameters and is computationally intensive. A simpler approach is to use equations that represent the most important processes of heat and mass transfer (Bolstad et al., 1997). This approach can be less accurate, resulting in a trade-off between model complexity and model accuracy (Gilad-Bachrach et al., 2003). A hybrid method is to use a simple theoretical structure as the foundation of the model and obtain empirical estimates of temperature to calibrate or fit the model to a desired system (Bryant and Shreeve, 2002; Cui et al., 2019; Hietaharju et al., 2018; Maclean et al., 2017; Singh and Tiwari, 2017). The hybrid approach can produce accurate results for systems that are measured, but the hybrid model cannot be extended to other systems without acquiring new empirical temperature measurements for calibration.

We developed a tree cavity thermal model that accurately predicts temperature within the tree cavity over time, has a tractable complexity that captures the main processes driving temperature within the tree cavity, is easily parameterized so it can be applied to many ecological questions, and is adaptable enough to be used in a range of conditions. The model uses ambient temperature and a small number of cavity-specific thermal and physical characteristics to predict the temperatures within tree cavities over

time. Our objectives were to: 1) define a tree cavity system by identifying the major processes of heat and mass transfer that influence cavity temperatures; 2) describe a thermal model that incorporates the major heat and mass transfer processes to estimate cavity temperatures; and 3) test the model's ability to accurately predict temperatures in tree cavities. We also tested the model's ability to predict temperatures in den boxes, which are functionally equivalent to natural tree cavities (Grüebler et al., 2014; Lindenmayer et al., 2009; Mänd et al., 2005; Maziarz et al., 2017; McComb and Noble, 1981a).

## **Methods**

### **Defining the cavity system**

Temperature within a cavity chamber varies over time as energy is constantly exchanged between the environment and the cavity. Thermal equilibrium is unlikely to be reached because of daily cycles in ambient temperature. Energy flow equations can account for a cavity's transient flow of energy through the use of partial derivatives (Potter and Andresen, 2002; Reid et al., 2020). An alternative approach is to treat cavity systems as a lumped capacitance reservoir of heat, which simplifies transient heat analyses by removing the space variable and allowing temperature to be predicted as a function of time alone, and assumes radiation and convection are negligible (Hietaharju et al., 2018; Hudson and Underwood, 1999; Kossak and Stadler, 2015). Using these simplifying assumptions, we can treat a tree cavity system as a lumped capacitance reservoir of heat with two main processes of heat and mass transfer occurring (Figure 1.1): 1) conductive heat ( $Q_{cond}$ ) transferred between ambient air and the cavity system;

and 2) the displacement of air and the associated heat ( $Q_{hole}$ ) through one or more entrance holes.

## **Cavity Model Description**

### ***Energy change equations***

The energy transfer rate (Watts) through any system is equal to the sum of the energy transfer rates in and out of the system. Equation 1 describes the energy transfer rate through a cavity system based on  $Q_{cond}$  and  $Q_{hole}$ :

$$1. \quad \frac{dQ_{cavity}}{dt} = \frac{dQ_{cond}}{dt} + \frac{dQ_{hole}}{dt}$$

where  $\frac{dQ_{cavity}}{dt}$  is the cumulative energy transfer rate through the cavity system,  $\frac{dQ_{cond}}{dt}$  is the conductive heat transfer rate between the ambient air and the cavity system, and  $\frac{dQ_{hole}}{dt}$  is the mass transfer rate of air moving through the entrance hole(s) of the cavity system.

Heat transfer between the ambient air and the inside cavity chamber is resisted by all sides of the cavity chamber except the entrance hole(s). A side is comprised of one or more layers of material (i.e. wood, bark, insulation). The conductive heat transfer through a single side of a cavity can be expressed as the product of the overall heat transfer coefficient of the side, the outer surface area of the side, and the difference between the ambient temperature and the temperature of air in the cavity:

$$2. \quad \frac{dQ_{cond}}{dt} = U_s A_s [T_a - T_{in}]$$

where  $U_s$  is the overall heat transfer coefficient of a side (W/m<sup>2</sup>K) and is calculated using the thermal conductivity, and thickness of each layer of the side (Bergman et al., 2011),  $A_s$  is the outer surface area of the side (m<sup>2</sup>),  $T_{in}$  is the internal cavity temperature (K), and  $T_a$  is the ambient air temperature outside the cavity (K). To account for conductive heat transfer through all sides of a cavity chamber, the heat loss coefficient  $U_s A_s$ , (W/K), can be calculated as the sum of the products of the overall heat transfer coefficients and surface areas of each side of the cavity (Kossak and Stadler, 2015):

$$3. \quad U_s A_s = \sum_{i=1}^n U_{s(i)} A_{s(i)}$$

where  $U_{s(i)}$  is the overall heat transfer coefficient of side  $i$  (W/m<sup>2</sup>K), and  $A_{s(i)}$  is the outer surface area of side  $i$  (m<sup>2</sup>).

The mass transfer rate of air moving through the entrance hole(s) of a cavity system (e.g., Eq. 4) is calculated from volumetric air flow into the cavity through the entrance hole(s), the density of the ambient air, the isobaric specific heat capacity of the ambient air, and the temperature difference between the internal air volume and the ambient air (Kossak and Stadler, 2015):

$$4. \quad \frac{dQ_{hole}}{dt} = (\dot{V}_{air} \times \rho_{air_a} \times C_{\rho,air}) [T_a - T_{in}]$$

where  $\dot{V}_{air}$  is the volumetric air flow into the cavity through entrance hole(s) ( $m^3/s$ ).  $\dot{V}_{air}$  is the product of the surface area of the entrance hole and the speed at which air is moving through it,  $\rho_{air_a}$  is the density of the ambient air ( $kg/m^3$ ), and  $C_{p,air}$  is the isobaric specific heat capacity of air ( $J/kgK$ ).

In a cavity system, heat, and mass transfer processes act on two separate heat sinks (Kossak and Stadler, 2015): the air volume in the cavity chamber, and the materials such as wood, bark, bedding material, or insulation that make up the cavity structure (Fig. 1). We accounted for heat and mass transfer through each of these sinks by re-expressing equation 1 as the sum of the energy transfer rate through the air volume and the energy transfer rate through the material volume:

$$5. \quad \frac{dQ_{air}}{dt} + \frac{dQ_m}{dt} = \frac{dQ_{cond}}{dt} + \frac{dQ_{hole}}{dt}$$

where  $\frac{dQ_{air}}{dt}$  is the energy transfer rate through the air volume in the system and  $\frac{dQ_m}{dt}$  is the energy transfer rate through the material volume.

### ***Modified energy change equations***

Equations 1-5 predict energy change of the cavity system over time. We can predict temperature change over time using the heat capacity ( $J/K$ ) of the air and the heat capacity of the materials (Hietaharju et al., 2018; Kossak and Stadler, 2015). We expressed the energy change ( $J$ ) of the air volume in the system as the product of the heat capacity of the air and the change in air temperature in the cavity chamber, with heat

capacity of air being equivalent to the product of the volume, density and isobaric specific heat capacity of the air mass:

$$6. \quad dQ_{air} = C_{air} \times dT_{in} = (V_{air} \times \rho_{air} \times C_{p,air}) \times dT_{in}$$

where  $C_{air}$  is the heat capacity of the air volume (J/K),  $dT_{in}$  is the change in air temperature in the cavity chamber (K),  $V_{air}$  is the volume of the air in the cavity chamber ( $m^3$ ),  $\rho_{air}$  is the density of air in the cavity chamber ( $kg/m^3$ ), and  $C_{p,air}$  is the isobaric specific heat capacity of air (J/kgK).

The energy change through a material volume is the product of the heat capacity of the material volume and the change in air temperature inside the cavity:

$$7. \quad dQ_m = C_m \times dT_{in}$$

where  $C_m$  is the heat capacity of the material volume (J/K). The cavity system, however, can be composed of several materials, with each material having its own heat capacity value. Because we are treating the cavity as a lumped capacitance system, the heat capacity of the material volume ( $C_m$ ) is calculated as the sum of the heat capacities of all materials in the cavity system, with the heat capacity of material  $i$  equal to the product of its specific heat capacity, its volume, and its density:

$$8. \quad C_m = \sum_{i=1}^n C_{m(i)} = \sum_{i=1}^n C_i \times V_i \times \rho_i$$

where  $C_{m(i)}$  is the heat capacity of material  $i$  (J/K),  $C_i$  is the specific heat capacity of material  $i$  (J/kgK),  $V_i$  is the volume of material  $i$  (m<sup>3</sup>), and  $\rho_i$  is the density of material  $i$  (kg/m<sup>3</sup>). Equation 5 can now be re-evaluated as:

$$9. \quad \left( C_m \times \frac{dT_{in}}{dt} \right) + \left( (V_{air} \times \rho_{air} \times C_{p,air}) \times \frac{dT_{in}}{dt} \right) = \frac{dQ_{cond}}{dt} + \frac{dQ_{hole}}{dt}$$

Equation 9 can be expressed as a first order differential equation, where air temperature in the cavity chamber at time  $t$  can be predicted using values of  $T_{in}$  and  $T_a$  at the previous time step ( $t - 1$ ):

$$10. \quad T_{in(t)} = T_{in(t-1)} + \frac{\Delta t}{(C_m + (V_{air} \times \rho_{air(T_{in(t-1)})} \times C_{p,air(T_{in(t-1)})}))} \left[ (U_W A_W [T_{a(t-1)} - T_{in(t-1)}]) \right] + \left( (\dot{V}_{air} \times \rho_{air(T_{a(t-1)})} \times C_{p,air}) [T_{a(t-1)} - T_{in(t-1)}] \right)$$

$T_{in(t)}$  is the estimated internal temperature (K) at the current time step ( $t$ ),  $T_{in(t-1)}$  is the estimated internal temperature (K) at the previous time step ( $t - 1$ ),  $T_{a(t-1)}$  is the ambient temperature (K) at the previous time step ( $t - 1$ ),  $\Delta t$  is the time interval (seconds) between  $t$  and  $t - 1$ . Because the density and isobaric specific heat capacity of air changes with air temperature,  $\rho_{air(T_{in(t-1)})}$  is the density of air (kg/m<sup>3</sup>) at  $T_{in(t-1)}$ , and  $C_{p,air(T_{in(t-1)})}$  is the isobaric specific heat capacity of air (J/kgK) at  $T_{a(t-1)}$ .  $C_m$

## **Model Evaluation**

### ***Field Data Collection***

We collected ambient and cavity temperature data at 22 cavities in the Superior National Forest and the Chippewa National Forest in Minnesota USA, and 21 cavities in the Manistee National Forest, Michigan USA. The cavities we measured were used by American martens (*Martes americana*) and fishers during previous radiotelemetry studies (Erb et al., 2015; Joyce, 2013; Sanders et al., 2017). Sampled cavities were selected from a sub-sample of cavities that was representative of all cavities previously used in each study area. We used a stratified random sampling design to select cavities to sample based on three strata for tree diameter and three strata for cavity hole height above ground. We constrained the final sample to be similar to tree species composition, tree diameter, and status (live or dead) of trees used by martens or fishers (Erb et al., 2015; Joyce, 2013; Sanders et al., 2017). Our final sample included cavities in quaking aspen trees (N = 12, *Populus tremuloides*), northern white cedar trees (N = 6, *Thuja occidentalis*), red maple trees (N = 3, *Acer rubrum*), and a paper birch tree (N = 1, *Betula papyrifera*) in Minnesota. We sampled cavities in oak trees (N = 15, *Quercus* spp.), bigtooth aspen trees (N = 2; *Populus grandidentata*), and sugar maple trees (N = 4, *Acer saccharum*) in Michigan. We sampled 29 cavities in live trees and 14 cavities in dead trees.

We also tested the model on 27 fisher den boxes (hereafter, artificial cavities) in the Superior National Forest and the Chippewa National Forest in northern Minnesota, USA. Artificial cavities were made from plywood or a combination of plywood and foam

insulation and were used in a fisher habitat improvement study in northern Minnesota (M. Joyce, Pers. Obs.).

For natural cavities, we measured each cavity using the entrance hole(s) as access point(s). We used a string with washers tied to the end to measure distance to the floor of the cavity, a length of 16-gauge wire to measure the distance to the ceiling of the cavity, a diameter tape to measure the diameter of the bole at cavity entrance height, and a tape measure to measure inside diameter, the thickness of the wood surrounding the inner cavity, and entrance hole height and width. We used these measurements to calculate internal air volume, the volume of wood and bark, the total surface area of the cavity, and the area of the entrance hole. We calculated these values by assuming the entrance hole is the shape of an ellipse and the internal shape of each natural cavity was a cylinder and that the thickness of wood around the cavity was uniform (Clement and Castleberry, 2013). Conductive heat transfer from the ambient air to the inner cavity space occurs through the ceiling of the cavity, the floor of the cavity, and the wall of the cavity. For calculation purposes we assumed all sides of the cavity had the same thickness and thermal properties. We assumed the bark layer had the same thermal properties as the wood layer. Wood density, specific heat capacity, and thermal conductivity of the cavity wood (Table 1.1) were estimated from literature values for each tree species (Dunlap, 1912; Hedlund and Johansson, 2000; Repola, 2006; TenWolde et al., 1988). Each cavity varied in its physical and thermal characteristics (Tables 1.2-1.3).

There were five different artificial cavity designs tested. Dimensions, design, and construction materials used were similar to those used for a previous fisher den box study (Davis and Horley, 2015). The materials of each artificial cavity included the

construction materials of the cavity and 13 cm of wood chip bedding material placed at the bottom of the internal cavity space. Construction materials included pine, aspen, or Douglas fir plywood and extruded polystyrene insulation (Owens Corning, Foamular 250, 1.9 cm, R-4). Four of the artificial cavity types had sides that were constructed of two layers of untreated plywood with polystyrene insulation between them. The fifth artificial cavity type had a single layer of treated plywood, 3.8 cm x 3.8 cm pine boards for an internal frame, and no insulation. Each artificial cavity had a 7.6 cm x 10.2 cm rectangular entrance hole. For each artificial cavity we measured internal cavity volume, total volume of materials, and thickness of each construction material. We used these measurements to calculate the internal air volume, the volume of the construction materials, and the total surface area of the cavity. Density, specific heat capacity, and thermal resistance values for plywood, pine boards, woodchips and insulation (Table 1.1) were estimated from literature values or obtained in the lab (Al-Ajlan, 2006; Asdrubali et al., 2015; Dunlap, 1912; Kamke, 1989; MacLean, 1941; Osanyintola et al., 2005; Ragland et al., 1991; TenWolde et al., 1988). Like natural cavities, each artificial cavity type varied in its physical and thermal characteristics (Table 1.4). The ½ inch aspen plywood, and 5/8 inch Douglas fir plywood cavities were stained to prevent rotting and moisture build-up.

Ambient and internal temperatures were measured at 30-minute intervals for each cavity using temperature loggers (HOBO® MX2201 or UA-001-64 pendant data loggers, Onset Computer Corporation, Massachusetts, USA). For both cavity types, ambient temperature loggers were hung at chest height or next to the cavity hole and were housed in white funnels to prevent the effects of wind and solar radiation. For natural cavities,

internal loggers were either hung ~ 5 cm above the bottom of the cavity with fishing line or placed on the bottom of the cavity if the logger could not be hung. Internal loggers were positioned ~ 5 cm above the bedding material in artificial cavities.

We did not measure the velocity of air moving through the entrance holes. Instead, we assumed air velocity within cavities and moving through the entrance hole was 0.1 m/s which is similar to the standard air velocity within houses (American Society of Heating, Refrigerating and Air Conditioning Engineers, 2010; International Standard, 2005).

The density of air at 1 atmospheric pressure decreases from 1.45 kg/m<sup>3</sup> at -30°C to 1.16 kg/m<sup>3</sup> at 30°C. Isobaric specific heat capacity of air varies from 1003 J/kg\*K at -30°C to 1005 J/kg\*K at 30°C. For our study, we used a constant air density value of 1.29 kg/m<sup>3</sup> (at 0°C) and constant isobaric specific heat capacity value of 1004 J/kg\*K (at 0°C) to fit the model. Using constant values of density and specific heat capacity of air simplifies model computation and has a small effect on model results because the overall heat capacity of air is several orders of magnitude less than the overall heat capacity of the materials.

Based on the cavity-specific physical and thermal parameters and site-specific ambient temperature measurements described above, we modeled the internal temperature of each cavity throughout its measurement period using equation 10. We used the first internal temperature measurement as the initial temperature value used for variable  $T_{in(t-1)}$ . Predicted temperature ( $T_{in(t)}$ ) was then calculated at 30-minute intervals ( $\Delta t = 1800$  seconds) throughout the rest of the monitoring period using modeled internal temperature and measured ambient temperature at time  $t - 1$ .

## Data Analysis

### *Assessing Model Accuracy*

We evaluated model accuracy using root mean squared error (RMSE). For each cavity, we calculated model error at each sampling interval as the difference between measured and modeled cavity temperature. Model error was used to calculate daily RMSE for each cavity and an overall RMSE for the entire deployment.

For analysis, we used three generalized estimating equation models (GEE,  $\alpha = 0.05$ ) to evaluate sources of error in the model. GEE allowed us to test the generalizability of the model while accounting for the temporal correlation between sampled days (Zeger and Liang, 1986). GEE model 1 assessed differences in daily RMSE as a function of cavity type (*cavityType*: Natural or Artificial cavity). GEE model 2 assessed differences in daily RMSE within artificial cavities as a function of artificial cavity types (*ArtificialType*: Artificial cavity types). GEE model 3 assessed differences in daily RMSE within natural cavities as a function of study area (*studyArea*), the total heat capacity of the materials (*Cm*), the total heat transfer coefficient of the cavity sides (*Uw*), total material volume (*matVol*), outer cavity surface area (*cavSA*), entrance hole area (*holeA*), total cavity diameter (*cavDia*), and average thickness of the wood that makes up the side of the cavity (*sideThickness*). Due to unequal sample sizes, we did not include tree species or tree condition as covariates within GEE model 3. We assessed collinearity between covariates with scatter plot matrices that included locally weighted smoothing and Spearman correlation coefficients. Preliminary analysis identified high collinearity between *subVol* and *cavSA* ( $r = 0.87$ ), *matVol* and *Cs* ( $r = 0.93$ ), and *cavDia* and

*sideThickness* ( $r = 0.74$ ). Therefore, we removed *matVol* and *cavDia* covariates from the model.

For all models, we assumed a Gaussian error distribution and an autoregressive correlation structure that allows higher correlation for daily RMSE values taken closer together than those taken further apart. We also used Tukey's Honest Significant Difference (Tukey's HSD,  $\alpha = 0.05$ ) as a post hoc analysis to make pairwise comparisons. We performed all analyses in R (Version 4.1.1), with package 'geepack' (Halekoh et al., 2006). We assessed assumptions of normality and equal variance using diagnostic plots (quantile-quantile plots, plots of residuals vs. predictor variables, and scale location plots). We also used Cook's distance plots to assess leverage from outliers. All models met requirements without the need for data transformation.

### ***Thermal Arrest Periods***

Preliminary results showed that thermal arrest periods occurred in natural cavities. A thermal arrest interval occurred when  $\text{abs}(T_{in(t)} - \text{model error})$  was less than  $1^\circ\text{C}$ . Thermal arrest periods occurred when there were  $\geq 2$  consecutive thermal arrest intervals. A day with a thermal arrest period was identified as a thermal arrest day. We selected a random subset of all thermal arrest periods identified by this method and manually inspected the predicted and modeled cavity temperatures to confirm a thermal arrest period had occurred.

We identified the ambient and modelled temperatures that were associated with the thermal arrest periods. Because the occurrence of thermal arrest periods are in part related to ambient temperature and the temperature in the tree, we assessed how ambient

and modelled temperature could be used as indicators for thermal arrest periods. We used temperatures between -1 and 1°C for the temperature range when freeze-thaw conditions could occur.

To test if these periods significantly affected daily RMSE, we added the fixed covariate, *ThermalArrest*, to GEE model 3 to evaluate differences in daily RMSE between thermal arrest days and days that were not thermal arrest days.

### ***Evaluating Bias***

We evaluated systematic bias in model results by calculating average daily bias for each sampled artificial cavity, and average daily bias across days that did not have a thermal arrest period and days that did within natural cavities. We also calculated bias for each thermal arrest period.

## **Results**

### **Assessing Model Accuracy**

We monitored natural cavities for 5,884 days (MN; 2,953, MI; 2,931), which is equivalent to 282,432 temperature measurements at 30-min intervals. Average sampling period for natural cavities was 137 (+/- 33 SD) days. Average ambient temperature ranged from -19.6°C (SD = 1.4°C) to 28.0°C (SD = 2.9°C) for natural cavities in Michigan, and from -30.1°C (SD = 15.6°C) to 27.2°C (SD = 8.8°C) for natural cavities in Minnesota. We monitored artificial cavities for 4,598 days (220,704 temperature measurements), with an average of 166 (SD = 75) days sampled per cavity. Average daily

ambient temperature ranged from  $-32.6^{\circ}\text{C}$  (SD =  $6.1^{\circ}\text{C}$ ) to  $29.1^{\circ}\text{C}$  (SD =  $10.7^{\circ}\text{C}$ ) for artificial cavities.

Natural cavities had an average RMSE of  $1.77^{\circ}\text{C}$  (SD =  $0.66^{\circ}\text{C}$ , range =  $0.42 - 3.65^{\circ}\text{C}$ ) across the full monitoring periods from both states. Artificial cavities had an average RMSE of  $1.02^{\circ}\text{C}$  (SD =  $0.45^{\circ}\text{C}$ , range =  $0.42 - 1.94^{\circ}\text{C}$ ). The model-predicted internal cavity temperatures were generally consistent with measured internal cavity temperature and followed daily oscillations in ambient temperature throughout each monitoring period (Figure 1.2 a-d). Tables 1.5, 1.6, and 1.7 summarize RMSE for each natural and artificial cavity sampled.

Average daily RMSE across all cavities (natural and artificial) monitored was  $1.20^{\circ}\text{C}$  (SD =  $1.03^{\circ}\text{C}$ ). Daily RMSE was lower for artificial cavities ( $0.83^{\circ}\text{C}$ , SD =  $0.63^{\circ}\text{C}$ , range =  $0.04 - 4.7^{\circ}\text{C}$ ) than for natural cavities ( $1.47^{\circ}\text{C}$ , SD =  $1.20^{\circ}\text{C}$ , range =  $0.05 - 12.56^{\circ}\text{C}$ ; GEE, Wald = 40.5,  $P < 0.001$ ).

For artificial cavities, there were significant main effects of box design (GEE,  $F_{4, 4593} = 7.5$ ,  $P < 0.001$ ). Daily RMSE was slightly higher in the uninsulated  $\frac{3}{4}$  inch Pine plywood cavity compared to the insulated  $\frac{3}{4}$  inch pine plywood cavity (Tukey's HSD,  $P < 0.001$ ) and compared to the insulated  $\frac{5}{8}$  inch Douglas fir plywood cavity (Tukey's HSD,  $P = 0.01$ ). Daily RMSE was slightly higher in the insulated  $\frac{1}{2}$  inch Aspen plywood cavity compared to the insulated  $\frac{3}{4}$  inch Pine plywood cavity (Tukey's HSD,  $P = 0.02$ ). Table 1.8 summarizes daily RMSE across artificial cavity types

For natural cavities, there were no significant main effects for study area (*studyArea*, Wald = 1.26,  $P = 0.26$ ), the total heat capacity of the materials ( $Cm$ ,  $\beta < 0.001$ , Wald = 0.346,  $P = 0.56$ ), the total heat transfer coefficient of the cavity sides ( $Uw$ ,

$\beta = -0.34$ , Wald = 1.59, P = 0.21), the outer surface area of the cavity (*cavSA*,  $\beta = -0.08$ , Wald = 0.46, P = 0.50), the entrance hole area (*holeA*,  $\beta = 27.7$ , Wald = 3.41, P = 0.06), or the average thickness of the wood on the side of the cavity (*sideThickness*,  $\beta = -3.24$ , Wald = 0.60, P = 0.44).

For natural cavities, 75% of sampled days (4413 days) had less than 2°C RMSE (Figure 1.3). These included days with thermal arrest periods and days that did not include thermal arrest periods. Of the 1471 days with RMSE greater than 2°C, almost half (716 days) were days with a thermal arrest period and about 20% (272 days) occurred within 48 hours after a day that contained the end of a thermal arrest period. The 483 days with RMSE greater than 2°C that were greater than 48 hours after a thermal arrest period ended occurred across a broad range of average ambient temperatures (mean = -5.23°C, SD = 16.1°C, range = -30.2 to 24.9°C). Overall, for natural cavities 92% of all sampled days either had RMSE less than 2 or were near or in a thermal arrest period, while 8% of all sampled days had RMSE greater than 2 outside of a thermal arrest period.

For artificial cavities, 95% of sampled days (4347 days) had less than 2°C RMSE (Figure 1.3). Days with RMSE greater than 2°C occurred across a broad range of average ambient temperatures (mean = 3.95°C, SD = 11.9°C, range = -26.3 to 24.3°C). Further, 46% of all days with RMSE greater than 2°C occurred in the artificial cavity without foam insulation, and 20% of all days with RMSE greater than 2°C occurred in the ½ inch Aspen plywood artificial cavity.

### **Thermal Arrest Periods**

There were 1843 thermal arrest periods over 2343 days identified in natural cavities (MI: 1036, MN: 807). In Minnesota, thermal arrest periods accounted for 11% of the intervals sampled, while in Michigan they accounted for 33% of the intervals sampled. On average thermal arrest periods lasted for 17 hours (median = 6, SD = 43.8 hours, range = 1 – 1234.5 hours) with 70% of all thermal arrest periods lasting less than 12 hours, 80% of thermal arrest periods lasting less than 20 hours, and 90% of thermal arrest periods lasting less than 48 hours.

Figure 1.4 provides examples of identified thermal arrest periods in natural tree cavities. Average thermal arrest period temperature was  $-0.11^{\circ}\text{C}$  (SD = 0.44, range = -0.99 to 0.98). Thermal arrest periods followed expected phase change dynamics, in that temperatures stabilized every time the cavity reached temperatures between  $-1$  and  $1^{\circ}\text{C}$ . In many cases, especially during long thermal arrest periods, ambient and modelled temperatures oscillated between positive and negative temperatures during the thermal arrest period (e.g. Figure 1.4c). The longest thermal arrest period lasted 1234.5 hours (~51 days), and ambient temperature oscillated between freeze-thaw temperatures 69 times, and modelled temperature oscillated between freeze-thaw temperatures 13 times. The number of oscillations decreased as period length decreased.

There were significant main effects for days that exhibited thermal arrest (*ThermalArrest*) (GEE, Wald = 9.87, P = 0.002). Days without thermal arrest periods had slightly lower RMSE ( $1.34^{\circ}\text{C}$ , SD =  $1.02^{\circ}\text{C}$ , range =  $0.06 - 8.11^{\circ}\text{C}$ ) than days with a thermal arrest period ( $1.68^{\circ}\text{C}$ , SD =  $1.39^{\circ}\text{C}$ , range =  $0.05 - 12.56^{\circ}\text{C}$ ). Nonetheless, most thermal arrest periods had low error. For example, 69% of days with a thermal arrest period had less than  $2^{\circ}\text{C}$  RMSE, and 87% of days with a thermal arrest period had less

than 3°C RMSE. In contrast, 79% of days without a thermal arrest period had less than 2°C RMSE, and 92% had less than 3°C RMSE.

We found that modelled temperature was a relatively strong indicator of thermal arrest periods. A thermal arrest period occurred on 88% of days when modelled cavity temperatures were between -1 and 1°C. Ambient temperature was a weaker indicator of when a thermal arrest period would occur. A thermal arrest period occurred on 63% of days when ambient temperatures were between -1 to 1°C. Cavity properties did not appear to affect the probability of a thermal arrest period occurring. Cavities with wood 5 to 10 cm thick had 66% of days with freeze-thaw ambient temperatures that had a thermal arrest period, while cavities with wood 10 - 15 cm thick had 60% of days with freeze-thaw ambient temperatures that had a thermal arrest period, and cavities with wood 15 - 20 cm thick had 66% of days with freeze-thaw ambient temperatures that had a thermal arrest period. When assessed across different cavity diameters, cavities with diameters within 25 - 40 cm, 40 - 55 cm, and > 55 cm had 65%, 54%, and 64% of days with freeze-thaw ambient temperatures that had a thermal arrest period, respectively. When assessed by cavity heat capacity, cavities with heat capacities between 40,000 - 80,000 J/K, 80,000 – 120,000 J/K, and >120,000 J/K had 66%, 63%, and 61% of days with freeze-thaw ambient temperatures that had a thermal arrest period, respectively.

### **Assessing Bias**

Average daily bias for artificial cavities was -0.06°C (SD = 0.30, range = -0.85 to 0.34). For natural cavities, average daily bias for days that did not have a thermal arrest period was 0.06°C (SD = 0.51, range = -1.13 to 1.40). Average daily bias for days that

did have a thermal arrest period was  $-0.49^{\circ}\text{C}$  (SD = 0.48, range = -1.40 to 0.34). Average daily bias for thermal arrest periods was  $-0.56^{\circ}\text{C}$  (SD = 1.84, range = -10.1 to 9.98).

## Discussion

The temperature in a cavity system is governed by complex interactions between energy transfer processes, ambient conditions, habitat characteristics, and physical and biological properties of the cavity. The model described in this paper simplifies these complex interactions into two main modes of energy transfer that can be calculated from only 8 input parameters. Despite the simplifying assumptions that the model is based on, the model accurately predicted cavity temperature for both natural and artificial cavities across relatively long periods and broad ambient temperature ranges. Our sampling period RMSE values were similar to RMSE values for more complex thermal models predicting the temperature within solid tree stems (Potter and Andresen, 2002; Reid et al., 2020). RMSE values were also similar to RMSE values for a complex thermal model used to predict microclimate temperature throughout snow and soil profiles (NicheMapR; Kearney and Porter, 2017, Fitzpatrick et al., 2019; Kearney, 2020; Kearney et al., 2014). Additionally, GEE analyses showed that our model performed consistently in cavities with different thermal and physical characteristics and across two study areas with different thermal conditions, suggesting the model can be applied to cavities in different tree species, different cavity sizes, and forest conditions. We also found little bias in error for both artificial and natural cavities, indicating that there were no systematic tendencies, such as effects of radiation and convection that caused differences between modelled and

measured temperatures. This further shows that the energy processes included in the model are likely the most important processes that govern cavity temperatures.

We found the model predicted temperatures in artificial cavities better than in natural cavities. Thermal arrest periods accounted for some of the error in natural cavities, but differences are also likely related to increased error when measuring the physical characteristics of natural cavities. For natural cavities, surface area and volume, for example, could not be measured as precisely as surface area and volume of artificial cavities. Because the model predicts temperature as a function of the physical and thermal characteristics of the cavity, any error in estimates of cavity characteristics could contribute to error in the model. Other simplifying assumptions, such as our assumption that each natural cavity was a perfect cylinder, or the ceiling and floor were the same thickness as the outer side, would contribute to model error for natural cavities. Future work could focus on methods that would allow more precise estimates of natural cavity characteristics. For example, accuracy could potentially improve by cutting down the cavities to obtain accurate measurements of the physical properties of cavities. However, given the concerns over availability of large trees with cavities (e.g., Lindenmayer et al., 2012), and that error was still reasonably low, non-destructive sampling methods are likely sufficient for parameterizing the model.

The uninsulated  $\frac{3}{4}$  inch Pine plywood cavity and the insulated  $\frac{1}{2}$  inch Aspen plywood cavity had slightly higher daily RMSE than the other cavity types and contributed to the highest number of days with greater than 2°C RMSE. Higher error in the uninsulated  $\frac{3}{4}$  inch Pine plywood cavity may be attributed to its lack of insulation, making it less thermally stable, and more prone to radiation or convection energy transfer

processes than the other artificial cavity types. Nonetheless, differences in RMSE were small among all artificial cavity types, indicating that error caused by differences in plywood thicknesses and plywood tree species were small relative to random effects such as sample size, location of boxes, sampling period length, or other factors that could affect RMSE.

Ambient temperatures were usually above freeze-thaw temperatures in previous studies in which tree cavity temperatures were monitored (Coombs et al., 2010; Isaac et al., 2008; Maziarz et al., 2017; Mersten-Katz et al., 2012; Wiebe, 2001). We expected thermal arrest periods to occur in our sampled cavities because ambient temperatures in Minnesota and Michigan cross the freeze-thaw boundary during the winter. Thermal arrest periods also occur in tree stems that do not have cavities, and are common in subterranean and subnivean microenvironments (Charrier et al., 2017; Cohen, 1994; Derby and Gates, 1966; Graf et al., 2015; Kearney, 2020; Kudriavtcev et al., 2016; Reid et al., 2020; Thompson et al., 2018; Zhang et al., 2020; Zhao et al., 2021; Zhou et al., 2018).

The thermal arrest periods we identified in tree cavities followed the fundamental dynamics of phase change described in previous studies (Graf et al., 2015; Zhao et al., 2021). When cavity temperatures reached freeze-thaw temperatures (between -1 and 1°C), a thermal arrest period began and temperatures in the cavity remained within freeze-thaw for extended periods of time. When a thermal arrest period ended, measured temperatures would then gradually return to expected temperatures in the absence of freeze-thaw temperatures.

Thermal arrest periods did not occur in artificial cavities. This could be because artificial cavities maintain drier microclimate conditions than natural cavities (Maziarz et al., 2017; McComb and Noble, 1981a) and therefore may not have enough water content for thermal arrests to occur. Construction materials, such as plywood, have a lower moisture content than green wood in standing trees (Skaar, 2012). The water repellent chemicals in wood preservatives would also result in drier conditions in artificial cavity walls.

The model presented in this study does not directly account for phase change processes at freeze-thaw temperatures, and therefore cannot predict thermal arrest periods. Consequently, days that had a thermal arrest period had higher daily RMSE and accounted for proportionately more days that had RMSE greater than 2°C. Differences in average daily RMSE between days that had a thermal arrest period and days that did not have a thermal arrest period were less than 0.4°C. There was also a large proportion (69%) of thermal arrest days with RMSE less than 2°C, indicating the model can produce acceptable results at the daily scale during freeze-thaw conditions.

Predicting thermal arrest periods would decrease model error under freeze-thaw conditions. Phase change dynamics in trees, however, are complicated by differences in structure, cells, and tissues within and between individual trees and tree species (Charrier et al., 2017; Lintunen et al., 2013; Reid et al., 2020; Zarrinderakht et al., 2021). Patterns are also influenced by other factors such as microclimate (i.e temperature and humidity), topography, or how much water or sap is in the system (Charrier et al., 2017; Graf et al., 2015). Reid et al. (2020), describe a model that can predict temperatures throughout tree stems using transient heat flow processes. In their model they account for phase changes

of water by assigning the sapwood a large pseudo-specific heat capacity when the cavity reaches a specific temperature interval in which phase change is expected to happen. In a simulation they found the model predicted a thermal arrest with little error (RMSE = 0.9°C). Adapting their technique to the model described in this paper could be useful but may be difficult given that the foundation of our model is based on lumped capacitance energy transfer and not transient energy transfer.

We used modelled and ambient temperatures to predict when a thermal arrest period would occur and how long the thermal arrest period would last. We found that modelled cavity temperatures could be an effective indicator of when thermal arrest periods occurred. Ambient temperature, however, were not. When ambient temperatures reached freeze-thaw conditions in trees without cavities, small trees tended to reach freeze-thaw temperatures more frequently than large trees (Reid et al. 2020). Trees greater than 50 cm diameter experienced freeze-thaw temperatures at tap depth only 15% of the total days with freeze-thaw ambient temperatures. In contrast trees less than 5 cm diameter experienced freeze-thaw at tap depth 95% of the days with freeze-thaw ambient temperatures. They suggested that lower proportions in large diameter trees result from increased wood volume buffering ambient temperatures and preventing inner sapwood from freezing. We expected cavities with thinner walls, in smaller diameter trees, and with a lower heat capacity would reach freeze-thaw temperatures more often due to their relative inability to buffer ambient temperatures, and store heat. Our results showed slightly higher proportions of days with freeze-thaw ambient temperatures that had a thermal arrest period when compared to Reid et al. (2020), but cavities with different wood thicknesses, diameter of the bole at cavity height, and overall heat capacity did not

affect the proportion of days with freeze-thaw ambient temperatures that had a thermal arrest period. The presence of a cavity chamber, or the flow of air through the entrance hole might over-ride the effects of cavity characteristics such as bole diameter.

The length of thermal arrest periods varied, but there was a positive relationship between period length and how many times ambient and modelled temperature oscillated between positive and negative temperatures. This indicates that continuous oscillations over the freeze-thaw allow the cavity to maintain freeze-thaw conditions, resulting in continuous phase changes of water or sap throughout the cavity system, and extended periods of thermal arrest.

Thermal arrest periods in cavities can affect cavity selection and animal thermoregulation. For example, if cavities remain stable around freeze-thaw while ambient temperatures rise above freeze-thaw, the thermal benefit of thermal arrest periods to animals is lower. Conversely, if ambient temperatures fall below freeze-thaw while a cavity is experiencing a thermal arrest in temperature, an animal would benefit by selecting that cavity. The effect of body heat from an animal would tend to make a cavity warmer. At temperatures slightly above freeze-thaw, the added body heat would delay or prevent a thermal arrest period. In contrast, at temperatures slightly below freeze-thaw, added body heat could increase the probability or alter the length of a thermal arrest period. Despite a large range and high standard deviation of bias values across the thermal arrest periods, the average bias across all thermal arrest periods was close to 0°C. This indicates that the net thermoregulatory cost of selecting a cavity that experiences multiple thermal arrest periods is close to zero.

The framework of this model may be useful for predicting the temperature of other enclosed microsites. For example, the temperature of hollow logs, squirrel dreys, or enclosed nests could potentially be estimated by treating them as a lumped capacitance reservoir of heat and using similar simplifying assumptions we used to model tree cavities. However, other energy processes may play an important role in these systems. Testing and verifying the model on these systems would be needed.

### **Conclusion**

The thermal model we describe in this paper fits the criteria for a useful microclimate model. It is computationally simple and relatively easy to parameterize. It was generalizable across two study areas, in different tree species, in different cavity sizes, and in artificial cavities. Although we tested this model in cavities used by martens and fishers, the ability of model to predict cavity temperatures across a relatively broad range of conditions should allow it to model temperatures in cavities that are used by other animal species. Further, the thermal model is a useful tool for ecological applications such as understanding animal response to cavity temperature. For example, researchers can use our model to directly compare the thermal environments in different cavities and understand how differences in cavity characteristics influence cavity selection by animals. Similarly, our model can be used to predict temporal changes in cavity temperatures, which can be important for understanding cavity use in response to changes in climate.

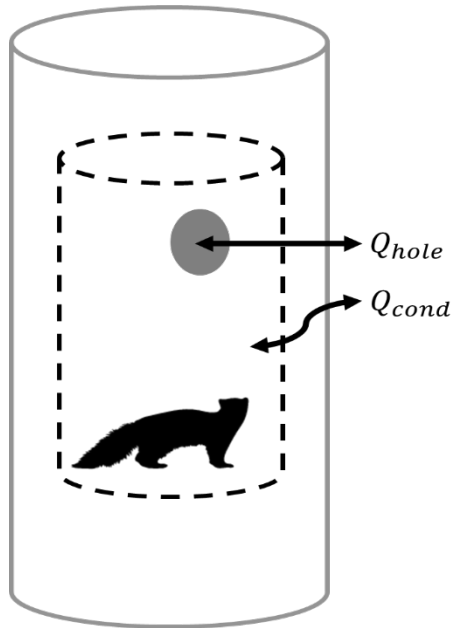


**Figure 1.1.** Schematic of the primary heat and mass transfer processes in a tree cavity system.  $Q_{cond}$  is the conductive heat transferred between ambient air and the cavity system, and  $Q_{hole}$  is the mass transfer of air through an entrance hole(s). Both  $Q_{cond}$  and  $Q_{hole}$  are expressed in joules (J).

**Table 1.1.** Density, specific heat, and thermal conductivity values used for estimating model parameters.

Material	Density (kg/m <sup>3</sup> )	Specific Heat (J/kgK)	Thermal Conductivity (W/mK)
Maple wood ( <i>Acer</i> spp.)	660	1369	0.18
Aspen wood ( <i>Populus</i> spp.)	410	1377	0.12
Oak wood ( <i>Quercus</i> spp.)	720	1361	0.19
Cedar wood ( <i>Thuja</i> spp.)	385	1357	0.09
Pine plywood ( <i>Pinus</i> spp.)	580	1369	0.10
Aspen plywood ( <i>Populus</i> spp.)	580	1369	0.10
Douglas fir plywood ( <i>Pseudotsuga menziesii</i> )	525	1360	0.12
Extruded polystyrene	33	1428	0.03
Woodchip bedding	196	1200	-
Pine boards ( <i>Pinus</i> spp.)	500	1200	-

**Table 1.2.** Summary of thermal and physical characteristics of sampled natural cavities in Superior National Forest and Chippewa National Forest in Minnesota.  $U_s A_s$  is the heat loss coefficient (W/K),  $C_m$  is the heat capacity of the material volume (J/K),  $V_{air}$  is the volume of air in the cavity chamber ( $m^3$ ), entrance hole area is the total area of all entrance holes into the cavity ( $cm^2$ ), side thickness is the average thickness of the wood and bark that makes up the side of the cavity, tree species is the species of tree the cavity is in. Tree species include Quaking Aspen (*Populus tremuloides*), Northern White Cedar (*Thuja occidentalis*), Paper Birch (*Betula papyrifera*), Red Maple (*Acer rubrum*), and Sugar Maple (*A. saccharum*).

Tree species	Cavity	$U_s A_s$	$C_m$	$V_{air}$	Entrance hole area	Side thickness
Quaking Aspen	1	4.8	88745	0.05	67.0	7.5
Quaking Aspen	2	3.9	141373	0.08	44.0	9.6
Northern White Cedar	3	3.4	50848	0.05	110.0	6.0
Northern White Cedar	4	2.0	188686	0.05	17.8	16.9
Paper Birch	5	1.7	55653	0.02	6.3	8.5
Northern White Cedar	6	1.2	61504	0.01	10.6	12.5
Northern White Cedar	7	2.7	41355	0.03	4.9	6.2
Northern White Cedar	8	1.8	72869	0.02	16.9	10.7
Quaking Aspen	9	3.6	78274	0.06	6.5	7.3
Quaking Aspen	10	2.1	91315	0.04	8.9	11.0
Red Maple	11	2.2	84015	0.04	12.8	10.4
Red Maple	12	5.8	152070	0.09	28.7	7.7
Red Maple	13	4.5	264641	0.05	6.5	13.7

**Table 1.2 (continued)**

Tree species	Cavity	$U_s A_s$	$C_m$	$V_{air}$	Entrance hole area	Side thickness
Quaking Aspen	14	2.0	44565	0.03	6.9	7.7
Northern White Cedar	15	1.8	115840	0.04	3.3	14.0
Quaking Aspen	16	2.2	82143	0.07	12.8	10.1
Quaking Aspen	17	1.7	89693	0.05	7.1	12.2
Quaking Aspen	18	2.1	123863	0.07	12.8	14.4
Quaking Aspen	19	7.0	897314	0.20	52.6	20.7
Quaking Aspen	20	1.1	92927	0.03	36.8	20.0
Northern White Cedar	21	3.6	254851	0.12	30.0	12.6
Sugar Maple	22	5.1	332695	0.11	41.0	14.2

**Table 1.3.** Summary of thermal and physical characteristics of sampled natural cavities in Manistee National Forest in Michigan, USA.  $U_sA_s$  is the heat loss coefficient (W/K),  $C_m$  is the heat capacity of the material volume (J/K),  $V_{air}$  is the volume of air in the cavity chamber ( $m^2$ ), entrance hole area is the total area of all entrance holes into the cavity ( $cm^2$ ), side thickness is the average thickness of the wood and bark that makes up the side of the cavity, tree species is the species of tree the cavity is in. Tree species include Oak (*Quercus* spp.), Quaking Aspen (*Populus tremuloides*), and Sugar Maple (*Acer saccharum*).

Tree species	Cavity	$U_sA_s$	$C_m$	$V_{air}$	Entrance hole area	Side thickness
Oak	1	4.1	179944	0.05	15.3	11.4
Oak	2	3.5	50620	0.03	5.9	6.3
Oak	3	4.1	108806	0.07	9.4	7.8
Quaking Aspen	4	1.5	87120	0.04	5.4	15.1
Oak	5	5.7	70305	0.04	12.4	5.1
Oak	6	2.1	132726	0.03	10.2	15.1
Quaking Aspen	7	2.4	80640	0.08	4.4	10.6
Oak	8	10.6	445297	0.33	6.5	10.3
Sugar Maple	9	2.5	147115	0.03	6.3	14.4
Oak	10	5.9	675827	0.47	40.1	19.3
Sugar Maple	11	4.1	108402	0.14	33.1	10.2
Sugar Maple	12	3.8	147608	0.07	20.4	10.9
Sugar Maple	13	2.2	80239	0.02	12.8	11.1
Oak	14	4.0	249118	0.05	7.2	13.7

**Table 1.3 (continued)**

<b>Tree species</b>	<b>Cavity</b>	<b><math>U_s A_s</math></b>	<b><math>C_m</math></b>	<b><math>V_{air}</math></b>	<b>Entrance hole area</b>	<b>Side thickness</b>
Oak	15	5.5	222004	0.11	7.3	10.5
Oak	16	7.2	981536	0.41	6.4	19.8
Oak	17	2.8	71847	0.05	3.9	9.0
Oak	18	6.9	347228	0.26	7.6	11.7
Oak	19	1.5	40786	0.01	9.4	9.5
Oak	20	6.3	713983	0.20	7.9	18.2
Oak	21	1.3	57346	0.02	10.2	12.1

**Table 1.4.** Summary of thermal and physical characteristics and design of artificial cavity types used for model validation. Insulated cavities contain Owens Corning, Foamular 250 insulation.  $U_s A_s$  is the heat loss coefficient (W/K),  $C_m$  is the heat capacity of the material volume (J/K),  $V_{air}$  is the volume of air inside (m<sup>2</sup>). Plywood thickness is the thickness of the plywood in cm.

<b>Cavity Type</b>	<b>N</b>	<b><math>U_s A_s</math></b>	<b><math>C_m</math></b>	<b><math>V_{air}</math></b>	<b>Plywood Thickness</b>
Insulated 3/4 in. Pine plywood	3	1.83	43937	0.064	1.79
Insulated 1/2 in. Pine plywood	4	1.94	29921	0.065	1.15
Insulated 1/2 in. Aspen plywood	7	1.82	29530	0.065	1.15
Insulated 5/8 in. Douglas fir plywood	9	1.81	30997	0.065	1.60
Uninsulated 3/4 in. Pine plywood	4	9.35	34217	0.111	1.79

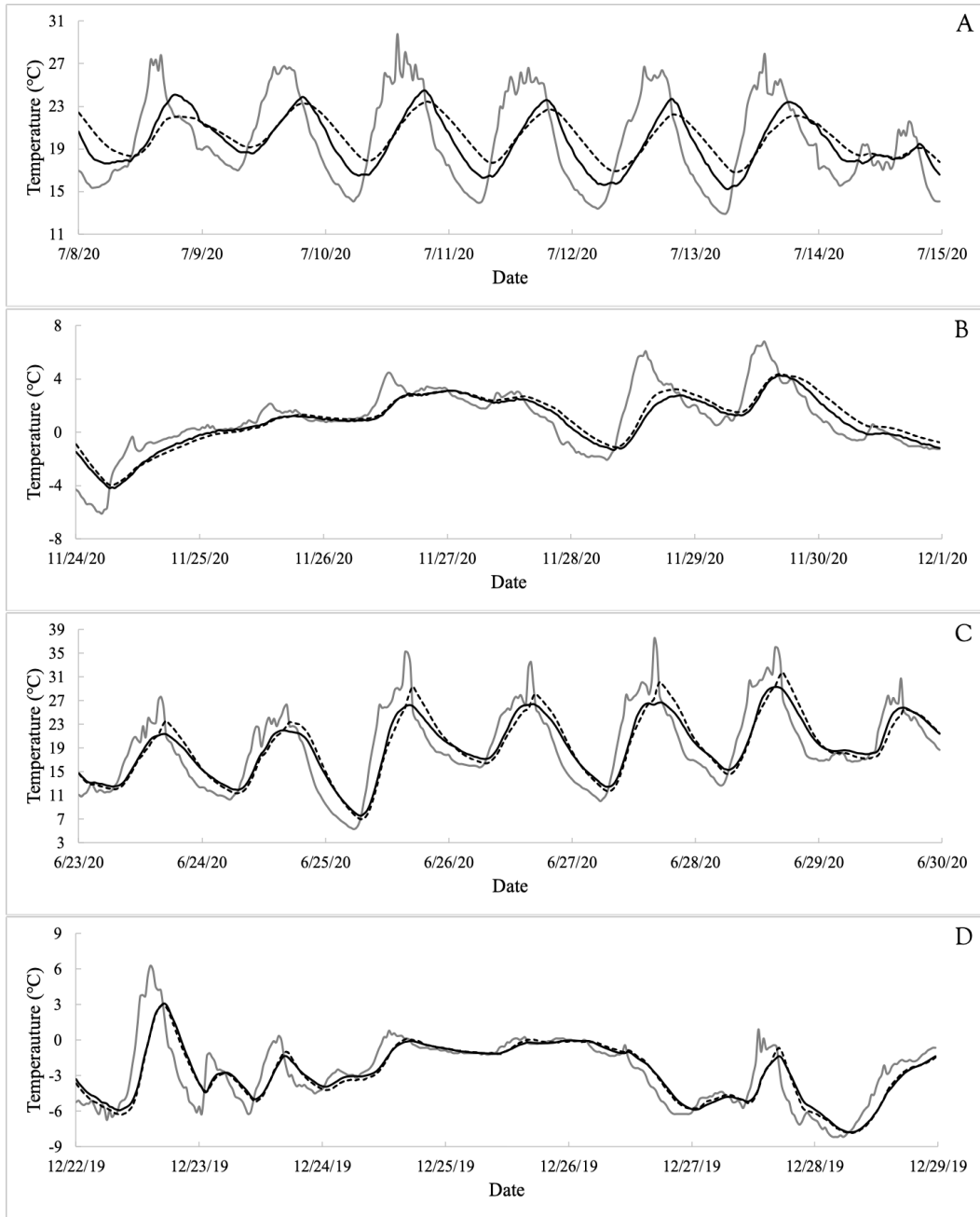


**Figure 1.2.** Results across a randomly sampled week in two natural cavities (A-B) and two artificial cavities (C-D). The solid gray line describes the ambient temperature. Measured temperature in the cavity is expressed with the solid black line. Modelled temperature is expressed as the dashed black line.

**Table 1.5.** Summary statistics for natural cavities sampled in the Superior National Forest and Chippewa National Forest in Minnesota, USA (root mean squared error RMSE and bias). Summary values of daily bias did not include days with thermal arrest periods.

Cavity	Number of days sampled	Sampling Period	Daily RMSE			Daily Bias			
			RMSE	Mean (SD)	Min	Max	Mean (SD)	Min	Max
1	213		1.40	1.03 (0.95)	0.06	5.37	0.12 (0.51)	-0.98	3.60
2	64		1.59	1.49 (0.53)	0.43	2.64	-0.50 (0.65)	-1.91	1.51
3	259		1.62	1.31 (0.94)	0.20	5.99	0.15 (0.49)	-1.41	1.21
4	103		2.20	2.08 (0.72)	0.49	3.85	-1.13 (1.16)	-3.44	2.26
5	155		1.42	1.23 (0.70)	0.18	3.55	0.15 (0.74)	-1.59	2.56
6	155		1.31	0.94 (0.90)	0.10	4.72	0.03 (0.43)	-1.85	2.60
7	155		2.17	1.80 (1.20)	0.24	5.49	0.91 (1.18)	-2.33	4.32
8	134		1.94	1.66 (0.99)	0.21	4.47	0.76 (1.15)	-1.96	4.41
9	85		0.65	0.55 (0.34)	0.11	1.40	-0.03 (0.31)	-0.98	1.09
10	120		1.51	1.22 (0.89)	0.13	4.00	0.06 (0.76)	-2.25	1.68
11	155		1.78	1.54 (0.89)	0.15	4.54	0.14 (1.28)	-3.45	3.36
12	131		1.67	1.42 (0.87)	0.24	3.54	0.47 (1.17)	-1.90	3.22
13	126		1.43	1.12 (0.88)	0.07	4.41	-0.24 (0.80)	-2.98	2.02
14	152		1.59	1.25 (0.97)	0.16	5.48	0.26 (0.73)	-1.99	3.64
15	156		2.22	1.94 (1.08)	0.14	4.76	0.45 (1.64)	-3.69	4.23
16	148		1.24	1.05 (0.65)	0.14	3.37	0.00 (0.63)	-1.76	1.40
17	120		1.15	0.92 (0.68)	0.08	3.71	0.21 (0.78)	-1.68	2.86
18	86		2.63	1.89 (1.84)	0.20	9.28	-0.20 (1.52)	-6.55	3.51
19	120		1.86	1.57 (1.00)	0.13	4.84	-0.20 (1.37)	-4.69	2.94
20	152		2.16	1.87 (1.07)	0.23	5.97	0.29 (1.24)	-2.54	2.53
21	103		1.62	2.08 (0.72)	0.49	3.85	-1.12 (0.94)	-3.53	1.53
22	61		1.22	1.09 (0.54)	0.28	2.66	-0.77 (0.72)	-2.43	1.04

**Table 1.6.** Summary statistics for natural cavities sampled in the Manistee National Forest in Michigan, USA (root mean squared error RMSE and bias). Summary values of daily bias did not include days with thermal arrest periods.

Cavity	Number of days sampled	Sampling Period RMSE	Daily RMSE			Daily Bias		
			Mean (SD)	Min	Max	Mean (SD)	Min	Max
1	147	0.81	0.68 (0.43)	0.06	2.34	-0.15 (0.38)	-1.25	0.62
2	103	2.57	2.25 (1.23)	0.30	5.15	0.49 (1.09)	-1.47	3.57
3	118	0.42	0.33 (0.25)	0.05	1.26	-0.20 (0.35)	-1.11	0.18
4	147	1.29	1.03 (0.77)	0.11	3.84	0.30 (0.90)	-2.53	3.24
5	110	1.65	1.44 (0.80)	0.28	4.61	-0.28 (0.45)	-1.19	1.11
6	147	1.11	0.95 (0.58)	0.09	3.58	-0.23 (0.56)	-1.65	0.90
7	148	2.67	2.13 (1.62)	0.19	8.02	-0.17 (2.20)	-7.99	4.66
8	147	1.83	1.40 (1.17)	0.08	7.77	-0.13 (1.55)	-7.66	3.54
9	148	2.50	1.97 (1.53)	0.23	9.00	0.40 (1.52)	-3.38	3.84
10	138	3.65	2.82 (2.32)	0.11	12.56	1.39 (3.29)	-8.03	6.60
11	138	2.71	2.25 (1.51)	0.19	7.72	0.85 (2.32)	-7.30	4.99
12	138	2.92	2.41 (1.64)	0.22	7.07	0.76 (2.63)	-5.92	6.97
13	138	1.52	1.13 (1.00)	0.15	4.83	0.08 (0.79)	-1.97	4.06
14	148	1.44	1.14 (0.87)	0.17	5.45	-0.07 (1.02)	-4.25	3.02
15	148	1.11	0.91 (0.62)	0.10	3.60	0.26 (0.72)	-3.15	1.88
16	148	2.33	1.84 (1.43)	0.10	9.47	-0.45 (1.50)	-4.72	1.94
17	148	2.28	1.86 (1.31)	0.23	7.39	-0.60 (1.53)	-7.22	2.24
18	148	2.53	2.06 (1.47)	0.27	9.07	0.65 (1.68)	-3.79	4.88
19	138	1.66	1.44 (0.83)	0.16	3.86	0.20 (1.32)	-2.65	3.73
20	138	0.95	0.75 (0.57)	0.10	2.57	0.14 (0.86)	-2.56	2.21
21	148	1.76	1.51 (0.89)	0.20	4.58	-0.62 (0.52)	-2.34	0.48

**Table 1.7.** Summary statistics for artificial cavities sampled (root mean squared error RMSE and bias). Nominal plywood thicknesses were ½ inch, 5/8 inch, and ¾ inch. Cavity type 1 is the insulated ¾ inch Pine plywood cavity. Cavity type 2 is the insulated ½ inch Pine plywood cavity. Cavity type 3 is the insulated ½ inch Aspen plywood cavity. Cavity type 4 is the insulated 5/8 inch Douglas Fir cavity. Cavity type 5 is the uninsulated ¾ inch Pine plywood cavity.

Cavity	Cavity Type	Number of days sampled	Sampling Period RMSE	Daily RMSE			Daily Bias		
				Mean (SD)	Min	Max	Mean (SD)	Min	Max
1	1	169	0.62	0.54 (0.29)	0.14	1.69	-0.27 (0.31)	-1.23	0.36
2	1	124	0.81	0.67 (0.45)	0.10	2.09	-0.43 (0.46)	-1.55	0.29
3	1	124	0.75	0.65 (0.37)	0.09	1.59	-0.42 (0.34)	-1.29	0.13
4	2	162	0.61	0.52 (0.31)	0.05	1.66	-0.15 (0.33)	-1.40	0.64
5	2	123	1.77	1.40 (1.08)	0.15	4.47	-0.85 (0.87)	-3.05	0.65
6	2	115	0.60	0.52 (0.28)	0.12	1.39	-0.19 (0.34)	-1.08	0.62
7	2	123	0.65	0.59 (0.26)	0.10	1.25	-0.08 (0.24)	-0.63	0.66
8	3	257	1.12	0.99 (0.51)	0.09	2.19	-0.05 (0.25)	-0.85	0.57
9	3	128	0.42	0.38 (0.17)	0.07	0.80	-0.02 (0.26)	-0.59	0.50
10	3	66	0.90	0.75 (0.48)	0.08	1.78	0.19 (0.35)	-0.60	1.23
11	3	220	1.01	0.88 (0.48)	0.05	2.60	0.19 (0.35)	-0.65	2.21
12	3	107	1.02	0.84 (0.56)	0.09	2.46	0.13 (0.29)	-0.87	1.01
13	3	50	0.80	0.70 (0.37)	0.15	1.35	0.25 (0.25)	-0.29	0.78
14	3	201	1.50	1.33 (0.69)	0.13	3.02	-0.09 (0.40)	-1.45	1.16
15	4	257	0.63	0.49 (0.38)	0.05	1.86	0.06 (0.20)	-0.73	0.63
16	4	257	1.94	0.64 (0.45)	0.06	1.93	-0.84 (0.88)	-2.52	0.59
17	4	357	0.63	0.54 (0.31)	0.03	1.37	0.14 (0.24)	-0.60	0.89
18	4	253	1.41	1.16 (0.79)	0.15	3.97	0.33 (0.41)	-0.65	1.53
19	4	114	0.92	0.74 (0.53)	0.10	2.37	0.01 (0.30)	-0.85	0.92
20	4	257	1.08	0.95 (0.51)	0.07	2.10	-0.09 (0.27)	-0.86	0.59
21	4	256	1.00	0.89 (0.43)	0.19	1.99	0.34 (0.33)	-0.67	1.36
22	4	256	0.61	0.52 (0.32)	0.07	1.74	-0.03 (0.21)	-0.78	0.67

**Table 1.7 (continued)**

Cavity	Cavity Type	Number of days sampled	Sampling Period RMSE	Daily RMSE			Daily Bias		
				Mean (SD)	Min	Max	Mean (SD)	Min	Max
23	4	128	0.64	0.54 (0.33)	0.06	1.50	0.04 (0.22)	-0.54	0.69
24	5	176	1.94	1.72 (0.90)	0.20	4.70	-0.08 (0.57)	-1.73	2.47
25	5	78	1.78	1.57 (0.84)	0.19	3.87	0.00 (0.39)	-1.29	0.96
26	5	117	0.82	0.75 (0.33)	0.11	1.61	0.06 (0.24)	-0.53	0.72
27	5	123	1.63	1.46 (0.71)	0.29	3.58	0.17 (0.35)	-0.71	0.98

**Table 1.8.** Summary of daily root mean squared error (RMSE) for five artificial cavity types tested.

<b>Cavity Type</b>	<b>Mean</b>	<b>SD</b>	<b>Min</b>	<b>Max</b>
Insulated 3/4 in. Pine plywood	0.62	0.38	0.10	2.09
Insulated 1/2 in. Pine plywood	0.75	0.69	0.05	4.48
Insulated 1/2 in. Aspen plywood	0.92	0.59	0.06	3.02
Insulated 5/8 in. Douglas fir plywood	0.73	0.52	0.04	3.98
Uninsulated 3/4 in. Pine plywood	1.41	0.83	0.12	4.71

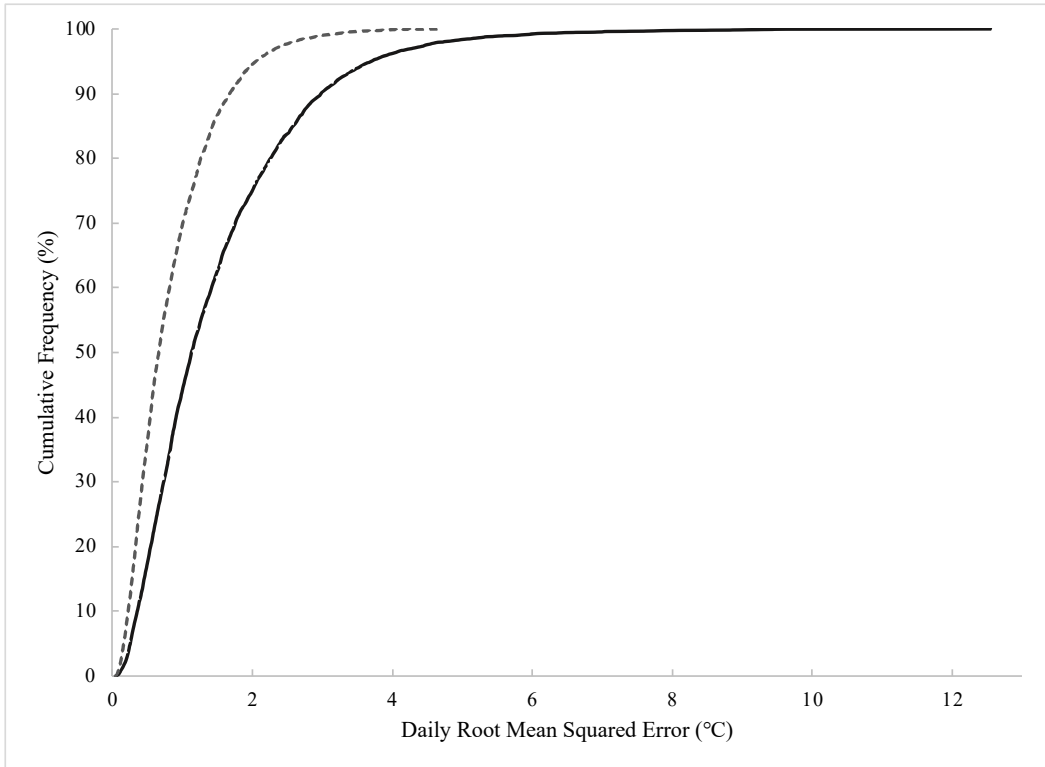


**Figure 1.3.** Cumulative frequency distribution of daily root mean squared error (RMSE) for natural (black line) and artificial cavities (dashed grey line) calculated across all cavities and all monitoring days.

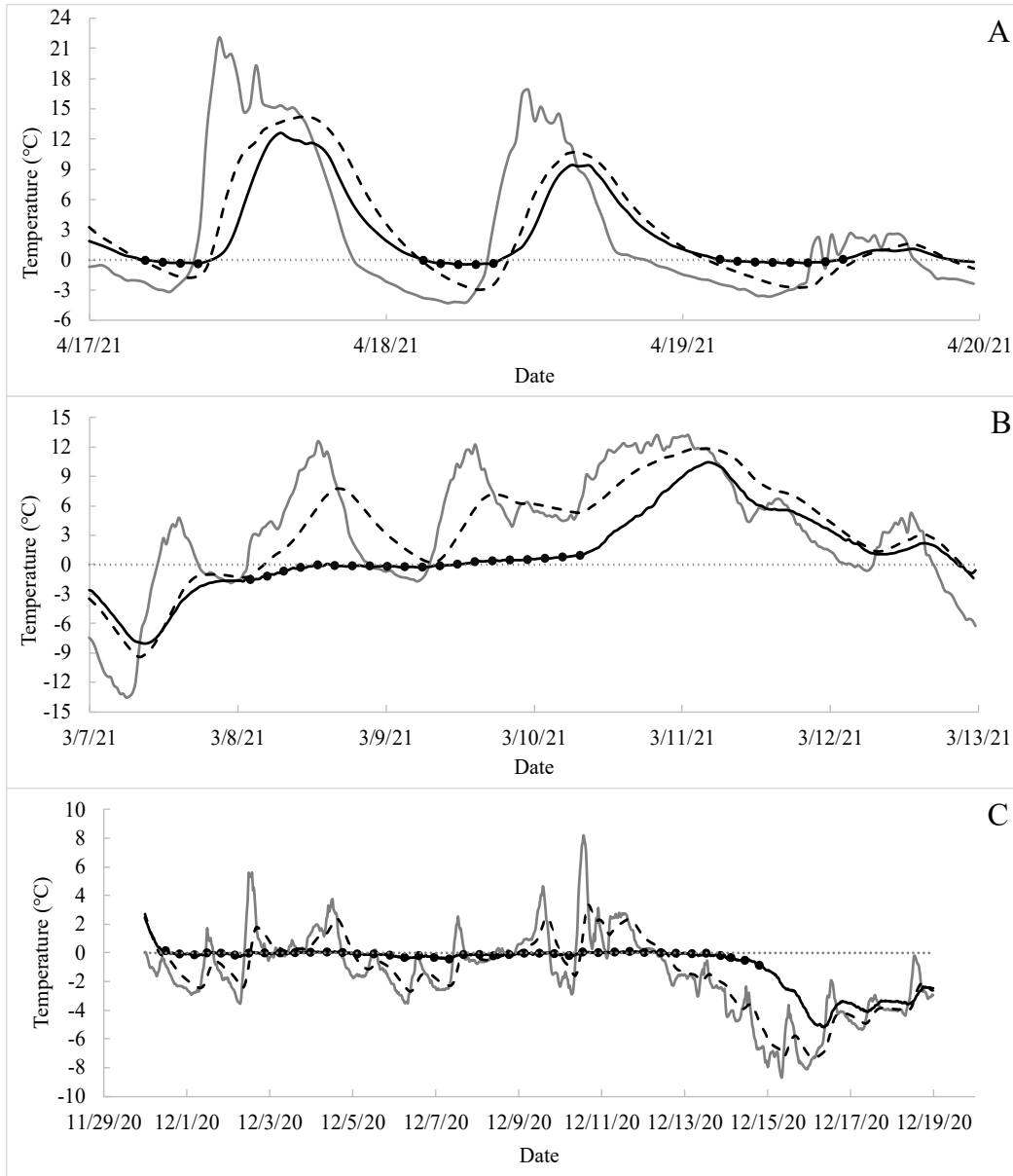


**Figure 1.4.** Multiple day results of natural cavities with thermal arrest periods at 0°C.

The solid gray line describes the ambient temperature. Modelled temperature is expressed as the dashed black line. Measured temperature in the cavity is expressed with the solid black line. The thermal arrest period(s) is expressed as the large dotted black line. The dotted grey line represents 0°.

Chapter 2: The role of ambient temperature and snowpack characteristics on American  
marten winter rest site selection in the Western Great Lakes Region

## Overview

Subnivean microsites are important rest sites for American martens (*Martes americana*) during the winter. With reduction in the spatial extent, temporal duration, and depth of snow cover from climate change, martens may be forced to use alternative microsites. In areas with shallow, transient snowpack, martens are using tree cavities. Whether tree cavities can provide the same energetic benefit, however, is not known. We evaluated the roles of ambient temperature, snowpack, tree cavity temperature, and subnivean temperature on marten winter rest site selection across the Western Great Lakes Region. Selection for tree cavities in lower peninsula Michigan, USA appears to be driven by shallow snow depths and warm ambient temps, by limited availability of subnivean microsites sites that would allow marten to benefit from the snowpack's insulation when present, or both. Conversely, deep snow and cold ambient temperature conditions make subnivean sites ideal for resting in Minnesota, USA. When snow is present and ambient temperatures are cold, subnivean sites are warmer and more energetically favorable than tree cavities in both study areas. However, as ambient temperatures increase and the availability of deep snow decreases with climate change, tree cavities could become a warmer and more energetically favorable site. Alternatively, subterranean sites could be an important ground level microsite that mimics above ground subnivean sites, if available.

## Introduction

Northern animals experience periods of cold temperatures and reduced food availability during the winter. Selection of microsites can reduce energy expenditure

associated with heat loss from the body to the environment (Williams et al., 2015). For example, many animals seek thermal refuge in the subnivium, a microsite at the snow-soil interface that provides warmer, more stable temperatures than the ambient air throughout winter when enough snow is present (Marchand, 2014; Pauli et al., 2013). Over the last few decades there has been a reduction in the spatial extent, temporal duration, and depth of snow cover as a result of climate change (Dye, 2002; Fountain et al., 2012; Groisman et al., 2004; Jylhä et al., 2008). Although climate change has created warmer winters, temperatures have likely not increased enough to offset the effect climate change has had on snow conditions (Pauli et al., 2013). As snow conditions continue to change, species that have relied on the subnivium for energy conservation may need to modify microsite selection and seek new thermal refuges. If these new thermal refuges provide less thermal protection, population declines, local extirpations, and northward range shifts could occur (Beever et al., 2017; Moritz and Agudo, 2013; Scheffers et al., 2014). Understanding how animals respond to changing snow conditions will help to predict effects of climate change on animal populations and help to develop strategies that can mitigate the negative impacts.

The American marten (*Martes americana*) is an ecologically, economically, and culturally important mammal species that occupies northern and high-elevation forests of North America (Buskirk and Ruggiero, 1994; Green, 2013). Thermoregulation is energetically costly for martens (Buskirk et al., 1988; Buskirk and Harlow, 1989; Flaherty et al., 2014; Harlow, 1994; Scholander, 1955; Yom-Tov et al., 2008). Martens survive during the winter using behavioral adaptations that include modifying activity

patterns, prey selection, and resting microsite selection (Harlow, 1994; Ruggiero et al., 1998; Zalewski, 2005).

Martens use various types of microsites for resting throughout the year. These include above-ground sites such as tree branches, witches' brooms, nests made by squirrels or birds, and tree cavities (Cockle et al., 2012; Joyce, 2013; Sanders et al., 2017; Slauson and Zielinski, 2009; Spencer, 1987). Resting sites at or below ground level include underground burrows, air space associated with coarse woody debris, root masses from tip-ups, and log piles (Joyce, 2013; Sanders et al., 2017; Spencer, 1987).

During the winter, martens rely on the thermal protection provided by the subnivium across most of their range. Temperature and thermal stability in the subnivium depend on the insulative capacity of the snow, which increases with snow depth and decreases with snow density (Ge and Gong, 2010). Deep snow conditions in most of the areas that martens occupy provide a stable environment that maintains a temperature of roughly 0 °C at the snow-soil boundary throughout the winter. It is because of these stable temperatures that martens choose subnivean sites as rest sites over other microsites during the winter (Buskirk et al., 1989; Joyce, 2013). If snow is not deep enough martens use other microsites, such as tree cavities, for resting (Joyce et al., 2017). However, tree cavities may not provide the same energetic benefit to martens as a functional subnivium would.

Throughout the Western Great Lakes region (WGLR) marten populations occupy a variety of forest types across a climate gradient that includes areas with deep and persistent snowpack and cold ambient temperatures, such as northern Minnesota, USA, and areas with a shallower, transient snowpack and warmer ambient temperature such as

the northern Lower Peninsula of Michigan, USA. Across this climate gradient marten use different rest site types. For example, marten populations in Minnesota and northern Wisconsin have followed the classical patterns of winter rest site selection by selecting ground-level sites within or under snowpack (Gilbert et al., 1997; Joyce, 2013). Recently, martens have increased use of tree cavities during winter in Wisconsin (J. Woodford, Wisconsin DNR, unpublished data). In contrast, marten populations in Michigan's northern Lower Peninsula primarily rest in tree cavities during the winter (Sanders et al., 2017).

Geographic variation in rest site types used is likely governed by differences in microsite temperatures, which are modulated by the local weather conditions (Taylor and Buskirk, 1994; Wilbert et al., 2000). In areas where martens use subnivean structures during the winter, martens will switch to rest sites in trees when snow is not present (Spencer, 1987; Bull and Heater, 2000; Joyce, 2013). This switch coincides with decreases in snow depths and increases in ambient temperatures during the spring and summer (Wilbert et al., 2000). Cavity temperatures fluctuate more than the subnivium, often mimicking the daily oscillations in ambient temperatures but are slightly more stable, reaching less extreme temperatures at the coolest and warmest parts of the day due to the insulation provided by wood and bark (Chapter 1; Coombs et al., 2010). Consequently, when snow is deep and ambient temperatures are cold, subnivean sites are warmer and more energetically favorable than tree cavities (Taylor and Buskirk, 1994). When snow depth decreases and ambient temperatures are warmer, however, subnivium sites are less stable and tend to follow daily oscillations in ambient temperature (Pauli et al., 2013; Taylor and Buskirk, 1994; Thompson et al., 2018).

We evaluated the roles of ambient temperature, snowpack, tree cavity temperature, and subnivean temperature on marten winter rest site selection. We focused on two study areas where previous studies on marten rest site selection were conducted: the Manistee National Forest (MNF) in the Lower Peninsula of Michigan and the Superior National Forest (SNF) in northeastern Minnesota. Within the study areas martens used several different rest site types including cavities in trees and snags, nests or witches brooms in the tree canopy, branches, and burrows accessed from various types of openings (Joyce, 2013; Sanders et al., 2017). In the SNF martens predominantly selected subnivean sites (69%) for resting during the winter (Joyce, 2013). In contrast martens primarily used tree cavities (70%) for resting in the MNF (Sanders et al., 2017). We hypothesized that martens in the SNF select subnivean sites because deep snow and cold ambient temperatures create subnivean rest sites that are warmer than the ambient air and other microsites, while martens in the MNF are likely using cavities during the winter because snowpack conditions do not allow a stable subnivium to form.

We had three specific objectives to assess differences in rest site selection between these two study areas. First, we tested whether differences in rest site selection could be explained by differences in snow depth and ambient temperature between the study areas. We used a decision tree model based on snow depth and ambient weather (Taylor and Buskirk 1994) to predict whether a marten should use a subnivean site, a tree cavity, or a tree branch site for resting. The model assumes that martens would use the warmest rest site type available based on the local snow depth and ambient weather conditions. We applied Taylor and Buskirk's model to compare model predictions to decisions made during actual resting events.

Our second objective was to compare snowpack depth, snow density, ambient temperatures, and microsite temperatures between tree cavities and subnivean sites within and between each study area. Differences in snowpack and ambient temperature conditions would affect both microsite temperature and availability of subnivean sites in the two study areas. Further, any differences in microsite temperatures within and between the two study areas could provide insight into why martens use more subnivean sites in the SNF and more tree cavities in the MNF, as well as help understand how martens will respond to increases in ambient temperature and changes in snowpack in the future.

Our third objective was to evaluate the energetic consequences of rest site selection. We used microsite temperatures and an energetic model to estimate the cost of being inactive in the different rest site types in each study area. The energetic cost of resting partly depends on when and how much time martens are active. Marten activity patterns are variable among individuals and populations based on sex, weather, and season. During the winter, martens decrease activity to help reduce their overall energy expenditure (Gilbert et al., 2009; Zalewski, 2000). In Wisconsin, Gilbert et al. (2009) found that American martens were active 4.8 hours per day (SD = 1.0) during winter. McCann et al. (2017) found that martens in Wisconsin had 3 (SD = 1) active bouts per day, with each active bout lasting 1.1 hours (SD = 0.8). Unpublished data from northeastern Minnesota found similar durations of activity during winter (J. Erb, Minnesota DNR, unpublished data). Another marten species, the European pine marten (*Martes martes*), is active about 6 hours per day in December and January (Males:  $6.1 \pm 2.4$  hours; Females:  $7.2 \pm 3.5$  hours) and 3 to 5 hours per day in February and March

(Males:  $4.6 \pm 2.1$  hours; Females:  $2.8 \pm 0.9$  hours) (Zalewski, 2000). When martens are active also varies. In California, marten activity patterns during the winter are relatively homogenous throughout the day and night but appear to be highest at sunrise and sunset in November-December, and highest during the day in January-February (Martin, 1987; Zielinski et al., 1983). In Minnesota, martens are generally nocturnal during winter, with peaks in activity between 19:00 and 05:00 (J. Erb, Minnesota DNR, unpublished data). In Poland, European pine martens are also nocturnal during the winter (Zalewski, 2001).

By addressing these objectives, we will improve understanding of the causes and consequences of winter rest site selection across the WGLR. If use of one type of microsite is more energetically costly during winter, higher use of that microsite may affect the ability of individuals to meet energy needs, which could affect population status or viability. Understanding the thermal differences in microsite types across the WGLR would help to predict how martens will respond to future changes in snowpack conditions, which allows us to assess vulnerability of martens to climate change and develop strategies for conserving thermal microsites.

## **Methods**

### **Study areas**

#### ***Superior National Forest, Minnesota***

We used the same study area described by Joyce (2013). The study area is in northeastern Minnesota ( $47^{\circ}30'N$ ,  $91^{\circ}52'W$ ) within the southcentral portion of the Superior National Forest (SNF). The area consists of four main forest cover types: mixed coniferous-deciduous forest (hereafter mixed-wood forests), lowland conifer, upland

conifer, and deciduous forest. Mixed-wood forests consist of aspen (*Populus tremuloides* and *P. grandidentata*), paper birch (*Betula papyrifera*), balsam fir (*Abies balsamea*), red maple (*Acer rubrum*), white pine (*Pinus strobus*), and white spruce (*Picea glauca*). Lowland conifer forests consist of black spruce (*P. mariana*), tamarack (*Larix laricina*), and white cedar (*Thuja occidentalis*). Upland conifer forests consist of red pine (*Pinus resinosa*) and jack pine (*P. banksiana*). Deciduous forests consist of aspen, paper birch, red maple, and sugar maple (*Acer saccharum*).

The study area in the SNF has an average winter (November to March) temperature of -7°C (SD = 6.4) (Figure 1). The area receives 184.6 cm (SD = 52.1) of snowfall annually, with average maximum snow depth of 63.2 cm (SD = 18.2) across the winter (Figure 2) (2010 – 2021 NOAA National Climatic Data Center Climate Data Online, <https://www.ncdc.noaa.gov/cdo-web/>).

### ***Manistee National Forest, Michigan***

Our Michigan study area is the same area described by Sanders et al. (2017). The study area is located in Michigan's northern lower peninsula (44°42'N, 85°40'W) in the Manistee National Forest (MNF). Currently, the study area consists of a variety of upland forest types such as mixed-hardwood, and second-growth conifer stands. Deciduous species include red oak (*Quercus rubra*), white oak (*Q. alba*), black oak (*Q. velutina*), black cherry (*Prunus serotina*), red maple, sugar maple, aspen (*Populus tremuloides* and *P. grandidentata*), American beech (*Fagus grandifolia*), American basswood (*Tilia americana*), white ash (*Fraxinus americana*), iron wood (*Carpinus caroliniana*), yellow

birch (*Betula alleghaniensis*), and witch hazel (*Hammamelis virginiana*). Conifer species include red pine, white pine, jack pine, and eastern hemlock (*Tsuga canadensis*).

The study area in the MNF has an average winter (November to March) temperature of  $-1.4^{\circ}\text{C}$  (SD = 4.9) (Figure 1). The area receives 304.8 cm (SD = 98.2) of snowfall annually, with average maximum snow depth of 47.5 cm (SD = 14.7) across the winter (Figure 2) (2010 – 2021 NOAA National Climatic Data Center Climate Data Online, <https://www.ncdc.noaa.gov/cdo-web/>).

### **Assessing marten selection based on snow depth and ambient temperature**

We tested whether martens in each study area were selecting sites based on snow depth and ambient temperature indicators described in Taylor and Buskirk's (1994) model. Taylor and Buskirk's (1994) model predicts that martens should select a subnivean site when the snow depth is deep ( $\geq 15$  cm) and the ambient temperature is cold ( $\leq -5^{\circ}\text{C}$ ). If snow depth is shallow ( $< 15$  cm) or if the ambient temperature is warm ( $> -5^{\circ}\text{C}$ ), martens should select cavities. In each study area, we compared predictions made by Taylor and Buskirk's model to rest site types selected by martens in the SNF and MNF (Erb et al., 2015; Joyce, 2013; Sanders et al., 2017). We calculated the percent of resting events that were correctly and incorrectly classified and described the ambient temperatures and snow depth conditions during the events.

In the SNF, martens used tree cavities 12 times and subnivean sites 68 times throughout the winter (November – April) (Erb et al., 2015; Joyce, 2013). In the MNF, martens used tree cavities 189 times and subnivean sites 4 times (Sanders et al., 2017). Subnivean sites in the SNF included sites that were in a subnivean air space directly

above the ground at the snow/soil surface, and burrows in the ground (Joyce, 2013), whereas subnivean sites in the MNF were strictly above the ground at the snow/soil interface (Sanders et al., 2017). We compiled snow depth and the average ambient temperature for the day the marten used each rest site to apply Taylor and Buskirk's model. If snow depth was measured when the rest site was found, we used the field-measured snow depth. Snow depth was not measured in the field for 24 resting events in the SNF and 11 resting events in the MNF. For these sites, we estimated snow depth using daily snow water equivalents and snow density values from the Snow Data Assimilation System (SNODAS) model (National Operational Hydrologic Remote Sensing Center 2004). We determined average daily temperature for each resting event using 4 x 4 km spatial resolution PRISM grid data (PRISM Climate Group, <http://prism.oregonstate.edu>).

### **Comparing snowpack, and ambient and microsite temperatures**

We monitored the ambient and internal temperatures of 17 tree cavities in the SNF and 21 cavities in the MNF using temperature data loggers (Chapter 1). We selected cavities to be representative of all cavities that were documented being used by martens in each study area (Joyce, 2013; Sanders et al., 2017). Measurements of ambient and internal temperature, and cavity characteristics for each cavity are described in Chapter 1. Data loggers were deployed in October and November 2020 and recorded data until late March or early April 2021.

In each study area, we measured ambient and subnivean temperatures at 6 sites. Sites were in either mixed-wood, deciduous, or coniferous forests, with 2 sites per forest

type per study area. Sites were randomly selected from the historical rest site locations in each cover type. At each site, we deployed 3 subnivean temperature data loggers (Onset Hobo MX2201), and 3 ambient temperature data loggers (Onset Hobo MX2201).

Ambient temperatures were recorded by data loggers housed in white funnels and hung about 1 m above the ground. Subnivean data loggers were set inside 3.8 cm PVC pipe that was wrapped in aluminum window screen material to prevent animal entry.

All temperature data loggers (cavity, ambient, subnivean) recorded temperatures every 15 minutes. We also estimated snow depth and snow density throughout the winter at each subnivean datalogger site we sampled in the SNF and MNF using the SNODAS model (Fitzpatrick et al., 2019). We compared average monthly snow depth, snow density, and ambient temperatures between the two study areas. We tested the effect of study area, month and the interaction between study area and month on each variable using two-way Analysis of Variance (ANOVA,  $\alpha = 0.05$ ). We included the interaction to test for differences in ambient temperatures between the two study areas within each month. We used Tukey's Honest Significant Difference (Tukey's HSD,  $\alpha = 0.05$ ) as a post hoc analysis to make pairwise comparisons for each month. Our period of comparison was when every site had data (11 November 2020 to 30 March 2021).

We compared monthly average tree cavity temperatures and monthly average subnivean temperatures from each study area. We tested the effect of two factors, microsite type ( $N = 4$ , subnivean and tree cavity microsites in both study areas) and month, and their interaction on temperature using two-way Analysis of Variance (ANOVA,  $\alpha = 0.05$ ). We included the interaction to test for differences in microsite temperatures between the four microsite types within each month. We used Tukey's

Honest Significant Difference (Tukey's HSD,  $\alpha = 0.05$ ) as a post hoc analysis to make pairwise comparisons for each month. Persistent snow cover and a corresponding subnivium was present in the Manistee study area from mid-December 2020 through mid-March 2021, and in the Superior study area from November 2020 through late-March 2021. We restricted monthly comparisons of subnivean and tree cavity temperatures to the date range where snowpack and a stable subnivean layer were present in both study areas.

Differences in ambient temperatures between the two study areas would cause differences in cavity temperatures. To verify that differences in cavity temperature are not caused by differences in the insulative capacity of the cavities themselves and that differences are solely caused by differences in ambient temperatures, we compared 6 cavity characteristics between the study areas using Student's t-tests ( $\alpha = 0.05$ ). The cavity characteristics we compared were important physical characteristics that influence heat flow and internal cavity temperatures (Coombs et al., 2010; Chapter 1): the volume of the cavity, the thickness of the wood and bark surrounding the cavity, the outer surface area of the cavity, the height of the inner cavity chamber, the diameter of the cavity bole, and the area of the entrance hole(s).

### **Estimating the energetic costs of rest site use**

We used an energy loss model (Appendix A) to estimate the amount of energy lost by a marten for one hour after it entered a resting microsite type using temperature conditions at the start of each hour. We calculated energy loss of an inactive female marten if it was in each microsite type using the empirical temperature measurements gathered in 2020-2021. We then averaged hourly energy loss for each sampling day and

each rest site type to estimate a standardized daily energy cost of the first hour in each rest site type. We used the hourly relative energy cost approach because we did not know how long a marten used a rest site, and temperature input values reflected unoccupied cavities and did not account for a marten raising the temperature of the cavity.

We used two-way Analysis of Variance (ANOVA,  $\alpha = 0.05$ ) to compare average energy loss at each microsite type within each area for each sampling month. We used one-way Analysis of Covariance (ANCOVA,  $\alpha = 0.05$ ) to compare the relationship between average daily ambient temperature and average hourly energy loss for each sampling day, and to test whether the relationship differed by microsite type (subnivium vs. tree cavity microsites). We also used one-way Analysis of Covariance (ANCOVA,  $\alpha = 0.05$ ) to compare the relationship between average daily snow depth and average hourly energy loss for each sampling day in the subnivium, and to test whether the relationship differed by study area (SNF vs. MNF). We restricted comparisons to the date range where snowpack and a stable subnivean layer were present in both study areas.

For all statistical tests we assessed assumptions of normality and equal variance using diagnostic plots (quantile-quantile plots, plots of residuals vs. predictor variables, and scale location plots). We also used Cook's distance plots to assess leverage from outliers. For comparisons of cavity characteristics between study areas, cavity volume and entrance hole surface area data did not meet normality assumptions. We ran t-tests for these covariates using both log-transformed and non-transformed data. Results were the same, so we reported results of the t-tests using non-transformed data. All other models met assumptions without the need for data transformation. We performed all analyses in R (R Core Team 2021; Version 4.1.1).

## Results

### **Assessing marten rest site selection based on snow depth and ambient temperatures**

In the Superior National Forest (SNF), martens used the microsite predicted by Taylor and Buskirk's model 46% of the time (37 out of 80 winter resting events). For most of these resting events (26), martens used the subnivium on days with deep snow and cold temperatures. Martens used cavities for the remaining resting events that were classified correctly, including 3 resting events when snow depth was shallow and temperatures were cold, 7 resting events when snow depth was shallow and temperatures were warm, and 1 resting event when snow was deep, but temperatures were warm.

Of the 43 resting events that were classified incorrectly in the SNF, there were 42 resting events (53% of all winter resting events) where martens used the subnivium, but the model predicted they should have used cavities. This included 20 resting events that occurred when snow depths were shallow and temperatures were cold, 9 resting events that occurred when snow depths were shallow and ambient temps were warm, and 13 resting events that occurred when snow depths were deep but ambient temperatures were warm. Additionally, there was 1 resting event where a marten used a cavity when the model predicted it should have used the subnivium. This event occurred when snow depth was deep and ambient temperature was cold.

In the MNF, martens used the microsite predicted by Taylor and Buskirk's (1994) model 85% of the time (164 out of 193 winter resting events). Martens used cavities for all these resting events, including 6 resting events that occurred when there was shallow snow and cold temperatures, 113 resting events that occurred when there was shallow

snow and warm temperatures, and 45 resting events that occurred when there was deep snow and warm temperatures.

Of the 29 resting events that were classified incorrectly in the MNF, there were 25 resting events (13% of all winter rest sites) where martens used cavities when the model predicted that they should have used the subnivium. Snow depth was deep, and ambient temperatures were cold for all these resting events. Additionally, there were 4 resting events (2%) where martens used a subnivean site, but the model predicted that they should have used cavities. Three of these resting events occurred when snow depth was deep, but ambient temperatures were warm, while the other resting event occurred when snow depth was shallow and ambient temperatures were warm.

### **Comparing snowpack and ambient and microsite temperatures**

Snowpack was present in the SNF until March 22, 2021 (Figure 3a). From mid-November to mid-December 2020, the MNF had a few short periods of snowpack, and then had persistent snowpack from 25 December 2020 to 11 March 2021. Snow was present on 97% of days sampled in the SNF, and 71% of days sampled in the MNF. There was a significant interaction between month and study area (two-way ANOVA,  $F_{4,51} = 20.4$ ,  $P < 0.001$ ), with snow depth being significantly deeper in the SNF compared to the MNF during November (Tukey HSD,  $P < 0.001$ ), December (Tukey HSD,  $P < 0.001$ ), and January (Tukey HSD,  $P < 0.001$ ). There was no significant difference in snow depth between study areas during February and March (Tukey HSD,  $P > 0.07$ ). In both study areas snow was deepest in February (SNF:  $30.4 \text{ cm} \pm 2.1$ , MNF:  $32.4 \text{ cm} \pm 2.3$ ) and shallowest in November (SNF:  $10.1 \text{ cm} \pm 0.69$ , MNF:  $1.6 \text{ cm} \pm 0.44$ ).

During periods of persistent snowpack, snow density increased as snow depth increased (Figure 3b). There was a significant interaction between month and study area (two-way ANOVA,  $F_{4,51} = 40.9$ ,  $P < 0.001$ ), with snow density being higher in the SNF than in the MNF across all months sampled (Tukey HSD,  $P < 0.001$ ). In both study areas snow density was highest in February (SNF:  $0.26 \text{ g/m}^3 \pm 0.004$ , MNF:  $0.21 \text{ g/m}^3 \pm 0.001$ ) and lowest in November (SNF:  $0.16 \text{ g/m}^3 \pm 0.003$ , MNF:  $0.07 \text{ g/m}^3 \pm 0.02$ ).

Ambient temperatures ranged from  $-29.2$  to  $8.5^\circ\text{C}$  in the SNF, and  $-13.0$  to  $14.3^\circ\text{C}$  in the MNF (Figure 3c). There was a significant interaction between month and study area (two-way ANOVA,  $F_{4,230} = 89.03$ ,  $P < 0.001$ ), with ambient temperature being warmer in the MNF than in the SNF across all months sampled (Tukey HSD,  $P < 0.001$ ). In both study areas ambient temperature was the coldest in February (SNF:  $-14.0^\circ\text{C} \pm 1.1$ , MNF:  $-6.7^\circ\text{C} \pm 0.49$ ), and warmest in March (SNF:  $0.91^\circ\text{C} \pm 0.80$ , MNF:  $4.4^\circ\text{C} \pm 0.92$ ). Average ambient temperature was below  $0^\circ\text{C}$  for 84% of days sampled in the SNF, and 64% of days sampled in the MNF.

The formation of a stable subnivium coincided with presence of a persistent snowpack in both study areas (Figures 3a,d). When a stable subnivium and persistent snow was present, subnivium temperatures ranged from  $-6.3$  to  $1.9^\circ\text{C}$  in the SNF, and  $-1.2$  to  $1.5^\circ\text{C}$  in the MNF (Figure 3d). When snow was not present ground-level temperatures were similar to ambient temperatures. This was apparent prior to and after the presence of persistent snowpack in the MNF. During periods of persistent snowpack, subnivean temperatures typically remained above ambient temperatures when ambient temperatures were below  $0^\circ\text{C}$ . Subnivean temperatures were colder than ambient temperatures in both study areas when ambient temperatures were above  $0^\circ\text{C}$ .

Differences in subnivean and ambient temperatures were less in the MNF due to ambient temperatures being closer to 0°C for most of the sampling period. In the SNF, subnivium temperatures were often less stable and would fall several degrees below 0°C despite the presence of relatively deep snowpack. For example, subnivium temperatures were several degrees below 0°C in February when snow depths exceeded 25 cm. These periods also corresponded with periods of cold ambient temperatures and high snow density. For example, subnivean temperatures in the SNF were coldest between 5 February and 21 February 2021, a period of extreme cold ambient temperature, high snow depth, and high snow density (Figure 3a-d).

Tree cavity temperatures ranged from -28.0 to 7.7°C in the SNF, and -12.2 to 11.7°C in the MNF (Figure 3d). Within each study area, cavity temperatures were less stable than the subnivium and followed daily oscillations in ambient temperatures. When ambient temperatures were relatively warm during the tail ends of the sampling period, tree cavity and subnivean temperatures were similar. Differences between tree cavity and subnivean temperatures were larger from mid-December 2020 to late February 2021 when ambient temperatures were cold (Figures 3a, c).

On average, tree cavities in the SNF provided the coldest microsite temperature across the entire winter (-9.6 °C, SD = 8.9, range = -38.4 to 22.4), followed by tree cavities in the MNF (-4.0 °C, SD = 4.2, range = -18.3 to 22.6), subnivean sites in the SNF (-2.2 °C, SD = 2.1, range = -11.2 to 0.91), and subnivean sites in the MNF (0.12 °C, SD = 0.60, range = -4.8 to 7.2). There was a significant interaction between month and microsite type (two-way ANOVA,  $F_{9,185} = 113.5$ ,  $P < 0.001$ , Figure 4). In December, subnivean microsites in the SNF and tree cavities in the MNF were the only microsite

types that did not differ in temperature (Tukey HSD,  $P=0.49$ ). All microsite types varied from one another in January and February (Tukey HSD,  $P < 0.001$ ). There was no difference in temperature between any microsite type in March (Tukey HSD,  $P > 0.07$ ).

Cavity characteristics in the MNF and the SNF were similar. There were no significant differences between the two study areas in cavity volume ( $t_{36} = 0.74$ ,  $P = 0.47$ ), wood thickness ( $t_{36} = 0.73$ ,  $P = 0.47$ ), outer cavity surface area ( $t_{36} = 0.22$ ,  $P = 0.83$ ), inner cavity height ( $t_{36} = -1.58$ ,  $P = 0.12$ ) and entrance hole area ( $t_{36} = -0.47$ ,  $P = 0.64$ ). Bole diameter at cavity height was slightly larger in the SNF ( $t_{36} = 2.42$ ,  $P = 0.02$ , Table 1).

### **Comparison of the energetic costs of microsite use**

The energy lost for the first hour a marten was in a rest site varied by rest site type and by study site. The predicted energy lost for the first hour in a rest site type over the entire winter for a female marten to use tree cavities in the SNF was highest (23.5 kJ, SD = 5.6, range = 11.4 to 37.0), followed by tree cavities in the MNF (19.5 kJ, SD = 2.6, range = 9.2 to 26.7), subnivean sites in the SNF (18.4 kJ, SD = 1.4, range = 16.7 to 23.7), and subnivean sites in the MNF (16.9 kJ, SD = 0.4, range = 14.5 to 18.4).

If a marten used the thermally best rest site each day of the 2020-2021 winter, 9% of rest sites would have been in cavities and 91% of rest sites would have been in the subnivean on the SNF. Similarly, 5% of rest sites would have been in cavities and 95% of rest sites would have been in the subnivean on the MNF. The energy cost of selecting the best rest site throughout the 2020-2021 winter would have reduced energy costs 22% compared to only choosing tree cavities in SNF, 14% less than only choosing tree

cavities in MNF, 0.7 % compared to only choosing subnivean microsities in the SNF, and 0.7 % compared to only choosing subnivean sites in MNF.

There was a significant interaction between month and microsite type on energy lost (two-way ANOVA,  $F_{9, 185} = 113.5$ ,  $P < 0.001$ , Figure 5). In December, all microsite types differed in energy lost (Tukey HSD,  $P < 0.01$ ), except subnivean sites in the SNF did not differ from tree cavities in the MNF (Tukey HSD,  $P = 0.49$ ). In January and February, all microsite types varied from one another (Tukey HSD,  $P < 0.001$ ). In March, there were no differences in daily energetic loss among microsite types (Tukey HSD,  $P > 0.07$ ).

Energy lost while inactive in subnivean sites (ANCOVA,  $t_{153} = -3.6$ ,  $P < 0.001$ ) and tree cavities (ANCOVA,  $t_{153} = -43.3$ ,  $P < 0.001$ ) decreases as ambient temperatures increases (Figure 2.6). We found a significant interaction between microsite type and ambient temperature (ANCOVA,  $t_{1, 304} = 23.9$ ,  $P < 0.001$ ), with slope being steeper for tree cavities. The ambient temperature at which there is no difference in energy lost is 1.7 °C. When temperatures are below 1.7 °C, martens save energy by resting in the subnivium. However, the amount of energy saved decreases as ambient temperatures approach 1.7 °C. When temperatures are above 1.7°C martens save energy by resting in tree cavities, with energy saved by using cavities increasing as ambient temperatures increase. When ambient temperatures are between -5 and 6°C there is a small difference (<16%) in energy lost between tree cavities and subnivean sites (Figure 2.6). Within this temperature range energy lost in tree cavities is variable and overlaps with energy lost in the subnivium.

There was no relationship between energy lost in the subnivium and snow depth in the MNF (ANCOVA,  $t_{76} = 0.3$ ,  $P = 0.76$ , Figure 2.7). Energy lost in the subnivium slightly increased with snow depth in the SNF (ANCOVA,  $t_{76} = -2.0$ ,  $P = 0.05$ ). We found a significant interaction between study area and snow depth (ANCOVA,  $t_{1,150} = 5.5$ ,  $P < 0.001$ ), with slope being slightly higher for the SNF. Of the days that had high energy loss at deep snow depths ( $\geq 15$  cm), 69% had an average ambient temperature that was less than or equal to  $-5^{\circ}\text{C}$ , and 42% had an average ambient temperature that was less than or equal to  $-15^{\circ}\text{C}$ .

## Discussion

Differences in marten rest site selection across the Western Great Lakes Region appear related to differences in local weather conditions that govern microsite temperatures. We predicted that selection for subnivean microsites is driven by relatively deep snowpack and cold ambient temperatures in the SNF. Taylor and Buskirk (1994) found that martens should select tree cavities when snow depth is less than 15 cm because the subnivium is not energetically favorable. However, martens in the SNF select subnivium sites despite snow depths being less than 15 cm (Erb et al., 2015; Joyce, 2013). The use of subnivium sites under shallow snow conditions could be related to the type of ground-level microsite martens use in the SNF, where 91% of the subnivean microsites were in an underground burrow (Joyce, 2013). Like snow, soil acts as an insulator and buffers ambient temperatures, with soil temperatures becoming warmer and more stable as depth increases (Florides and Kalogirou, 2005; Popiel et al., 2001). If snowpack is limited or not present, martens may be able to use subterranean microsites

and gain similar thermal benefits as if they used a subnivean microsite. Models such as NicheMapR (Kearney and Porter, 2017) could be used to predict below-ground temperatures at various depths, however, the depth and characteristics of subterranean sites used by martens are largely undescribed, making it difficult to evaluate thermal conditions in subterranean sites. Taylor and Buskirk's model, which was developed in an area where subnivean rest sites used by martens are within airspace in the snowpack, could be modified to include the conditions when subterranean burrows provide warmer, more favorable microsites. Because martens use subterranean rest sites in other areas (Buskirk, 1984; Spencer, 1987), this change would generalize the model to better represent marten rest site selection. Additional work is needed to better understand subterranean microsite use and to evaluate subterranean microsite temperatures and their impact on thermoregulation, especially in response to future climate change where loss of snowpack could reduce the suitability of subterranean sites during winter.

Above-ground subnivean microsites could also be beneficial at shallower snow depths. We found that thermal stability in the subnivium corresponded with the onset of accumulating snowpack, and that the subnivium was warmer than tree cavities at snow depths as shallow as 3 cm. Other studies found that stable subnivean temperatures can be maintained under depths as shallow as 5 cm (Thompson et al., 2018). At shallower snow depths, however, other factors such as ambient temperature and snow density play a more important role on thermal stability in the subnivium. Thompson et al. (2018) found that when snow depths are less than or equal to 10 cm, the subnivium is prone to larger temperature swings as snow density decreases and across a broader range of ambient temperatures. Snow must be deep enough to allow the formation of an air pocket large

enough for martens to rest in. A lower threshold snow depth, for example, 10 cm, would be a more reasonable threshold for predicting whether a marten is more likely to use the subnivium in the upper Midwest, especially when considering layers of leaf litter and duff that both act as additional layer of insulation at the snow-soil interface.

When snow was present, cold ambient temperatures created relatively large differences in temperature and energy loss between cavities and subnivean microsites for most of the 2020-2021 winter, with subnivean sites being more energetically favorable. Selecting tree cavities under cold conditions would likely lead to a substantial increase in the amount of time spent foraging to balance the additional thermoregulatory costs throughout the winter, which could challenge martens' ability to decrease activity and reduce their overall energy costs during the winter (Gilbert et al., 2009; Martin et al., 2020; Thompson and Colgan, 1994). Martens in the SNF, however, unexpectedly used subnivean rest sites at times when air temps were warm enough ( $> -5$  °C) that cavities should have provided a warmer microsite. There are ambient temperature conditions where small differences in energy lost among microsite types suggest there should not be strong selection for either microsite type. For example, we found that the difference in energy lost between tree cavities and subnivean sites is relatively low when ambient temperatures are between  $-5$  to  $6$  °C. This is likely in part the result of tree cavities exhibiting thermal arrest periods when ambient temperatures reach freeze-thaw conditions (Chapter 1). Therefore, factors other than energy conservation could also be affecting decisions on where to rest when ambient temperatures are between  $-5$  and  $6$ °C.

We found that microsite selection in the MNF is mostly driven by shallow snowpack and warm ambient temperatures. If snow is absent, martens should prefer

elevated positions, like tree cavities, for resting (Spencer, 1987; Bull and Heater, 2000; Joyce, 2013). A large portion (42%) of tree cavity resting events in the MNF occurred on days with no snowpack (Sanders et al., 2017). When snow is not present, ground temperatures follow daily oscillations in ambient temperature, whereas cavity temperatures are less variable because of their ability to buffer ambient temperature. Although ambient temperatures are warmer during the day and warming by solar insolation could make ground resting more thermally beneficial, martens would benefit from the insulation and overall protection from predators while in tree cavities (Zalewski, 1997b). Because the temporal duration of snowpack in the MNF is 26% shorter than the SNF (SNODAS 2008-2014, 2020-2021), it is likely that martens are, in part, selecting tree cavity sites more frequently in the MNF than the SNF because the overall lack of snowpack throughout the winter season would lead to higher energetic costs at night and predation risk if they were to rest on the ground.

The MNF still maintains moderate to deep snow conditions during a relatively large portion of the winter season. Like the SNF, results of 2020-2021 suggest that when snow is present, martens should be selecting subnivean microsites over tree cavities in the MNF because they were warmer and more energetically favorable. Consequently, we expected more subnivean microsite use when snow was present during the Sanders et al. (2017) study. The MNF's warm ambient temperature in part drives selection for tree cavities during periods of consistent snowpack. Differences in energy lost between tree cavities and subnivean microsites in 2020-2021 were relatively low in the MNF compared to the SNF. It was consistently warmer in the MNF, with 66% of days sampled being warmer than  $-5^{\circ}\text{C}$ . Under these warmer conditions, there is little difference in

energy lost between subnivean and tree cavity temperatures. Tree cavities also become more favorable when temperatures are above 6°C. Therefore, it is possible that martens selected tree cavities over subnivean microsites during the Robert et al. (2017) study because the differences in energy lost between the microsite types were likely not large enough to cause a significant increase in their daily energy budgets.

Selection for tree cavities in the MNF during periods where martens should be selecting subnivean sites could also be related to microsite availability. Martens need to have a microsite to rest in to take advantage of the insulation provided. Subnivean microsites are typically associated with coarse woody debris (CWD), where brush piles and logs help create air pockets in the snow for martens and other animals to rest in (Buskirk et al., 1989; Corn and Raphael, 1992; Martin et al., 2021; Petty et al., 2015). In the SNF and other areas, there is an abundance of coarse woody debris which allows for martens to select subnivean microsites below or above the ground surface (Buskirk et al., 1989; Joyce, 2013). In the MNF, CWD was historically limited throughout the area (Sanders et al., 2017). Further, martens in the MNF did not use underground burrows (Sanders et al., 2017).

Although we do not know how tree cavity availability differs between the two study areas, tree cavities could also be more readily available in the MNF than the SNF. Higher tree cavity abundance would decrease search and travel time, which would reduce the overall energetic cost of selecting a tree cavity. This could offset the energetic consequences of selecting tree cavities instead of slightly warmer and more energetically favorable subnivean sites in the MNF.

We suggest minor modifications to the snow depth and ambient temperature thresholds described by Taylor and Buskirk (1994) to generalize the model geographically (Figure 2.8). First, if snow depth is greater than or equal to 10 cm, and ambient temperature is between -5 and 6°C, a marten could choose either rest site type. Martens should use tree cavities if ambient temperature is greater than 6°C, and martens should choose subnivean sites if snow depth is greater than or equal to 10 cm, and ambient temperature is less than or equal to -5°C. Subterranean sites are still not explicitly accounted for in the modified model, although the reduced snow depth threshold could be viewed as implicitly including resting events when a marten used a subterranean site. These modifications could be more useful for predicting microsite use based on snow depth and ambient temperature conditions. For example, using the modified model about 69% of SNF rest sites were classified correctly, compared to 46% of SNF rest sites being classified correctly using the unmodified Taylor and Buskirk model. We could not test the modified model on the MNF rest sites because snow depth was recorded categorically as above or below 15 cm (Sanders et al. 2017).

### **Implications of future climate changes**

By 2100, average annual temperatures in the US Great Lakes Region are projected to increase 3-5°C, with increases in winter and spring precipitation of 20-30% (Hayhoe et al., 2010; Stocks et al., 1998). With rapid changes in snowpack conditions and warming ambient temperatures, martens may be forced to use alternative rest sites in areas such as the SNF which have historically experienced deep snowpack and cold ambient temperatures.

Results from this study show that tree cavities can be an important alternative rest site. We found that tree cavities in the MNF had similar energetic costs to subnivean sites in the SNF. This, coupled with the fact that tree cavities in both study areas did not differ in their overall physical characteristics, indicates that if snowpack and ambient temperature conditions in the SNF become more similar to conditions in the MNF, martens can select tree cavities without experiencing a significant change in energy cost in rest sites.

With increased snow loss and increases in ambient temperature, martens would need to increase use of tree cavities as a thermal refuge during the winter. Natural decay, natural disturbances, and forest harvest by humans, however, have decreased the global distribution and abundance of tree cavities (Graves et al., 2000; Remm and Löhmus, 2011). Increased dependence on tree cavities will also likely lead to increased competition for suitable cavities for resting and reproduction. In response, rapid and effective strategies could be needed to increase the availability of tree cavities for animals. For example, changes in forestry practices could be used to preserve old growth forests and maximize the potential for trees to become large enough to form cavities, especially in second-growth forests (Fan et al., 2005, 2003; Kenefic and Nyland, 2007; Lammertink et al., 2019). Alternatively, wildlife managers can deploy nest boxes in forest stands that lack available cavities (Croose et al., 2016; Delheimer et al., 2018).

Even if martens have access to tree cavities to offset energetic costs of losing snowpack, loss of snowpack could still have negative consequences for martens and the communities in which they live. The loss of the subnivium can increase seed removal and decrease plant and seed viability. This affects masting and plant-herbivore dynamics, and

ultimately predator-prey dynamics within a forest ecosystem (Guiden et al., 2019; Guiden and Orrock, 2021; Zhu et al., 2019). Loss of subniveum would also directly affect many small prey mammals that depend on the subniveum for a safe thermal refuge throughout the winter (Kausrud et al., 2008; Williams et al., 2015; Zuckerman and Pauli, 2018). Further, changes in abundance of prey populations as a result of snow loss could indirectly disrupt predator-prey relationships and affect the distribution and energetics of predators, such as martens (Pauli et al., 2013; Zuckerman and Pauli, 2018).

### **Conclusion**

Selection for tree cavities in the MNF is driven, in part, by shallow snow depths and warm ambient temperatures, and probably by limited availability of subnivean microsites that would allow martens to benefit from the snowpack's insulation when present. Conversely, deep snow and cold ambient temperature conditions have made subnivean sites an important microsite for resting in the SNF. When snow is present and ambient temperatures are cold, subnivean sites are warmer and more energetically favorable than tree cavities in both study areas. With increases in ambient temperatures and decreases in snow depth, though, cavities become equally beneficial. Hence there is a need for considering conservation strategies that increase the tree cavity availability in the face of rapid climate change.

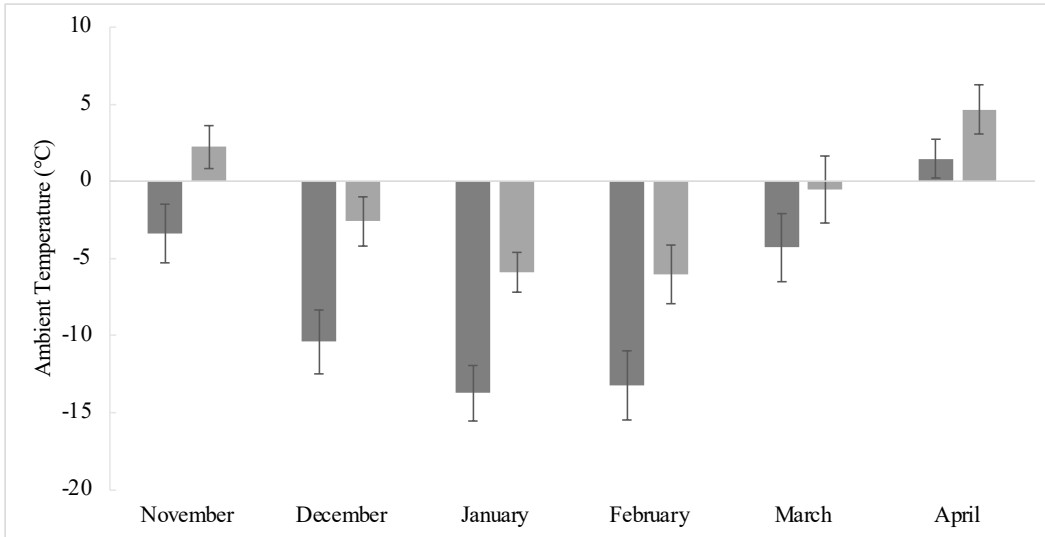


**Figure 2.1.** Winter ambient temperatures (November – March) in the Superior National Forest, Minnesota USA (dark gray), and the Manistee National Forest, Michigan USA (light gray). Each bar represents the average ambient temperature from 2010-2021. Error bars represent the 95% confidence intervals.

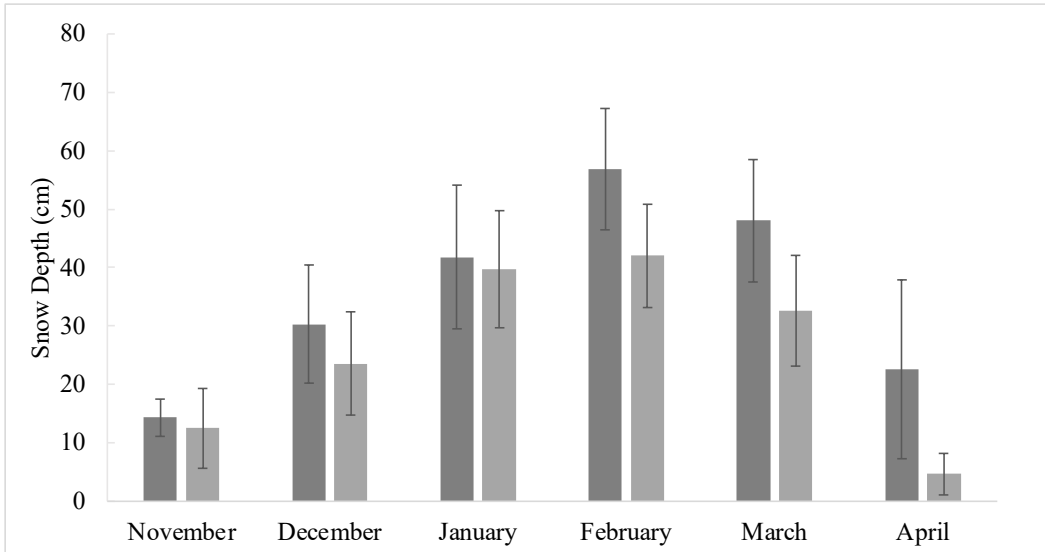


**Figure 2.1.** Winter snow depth (November – March) in the Superior National Forest, Minnesota USA (dark gray), and the Manistee National Forest, Michigan USA (light gray). Each bar represents the average snow depth from 2010-2021. Error bars represent the 95% confidence intervals.

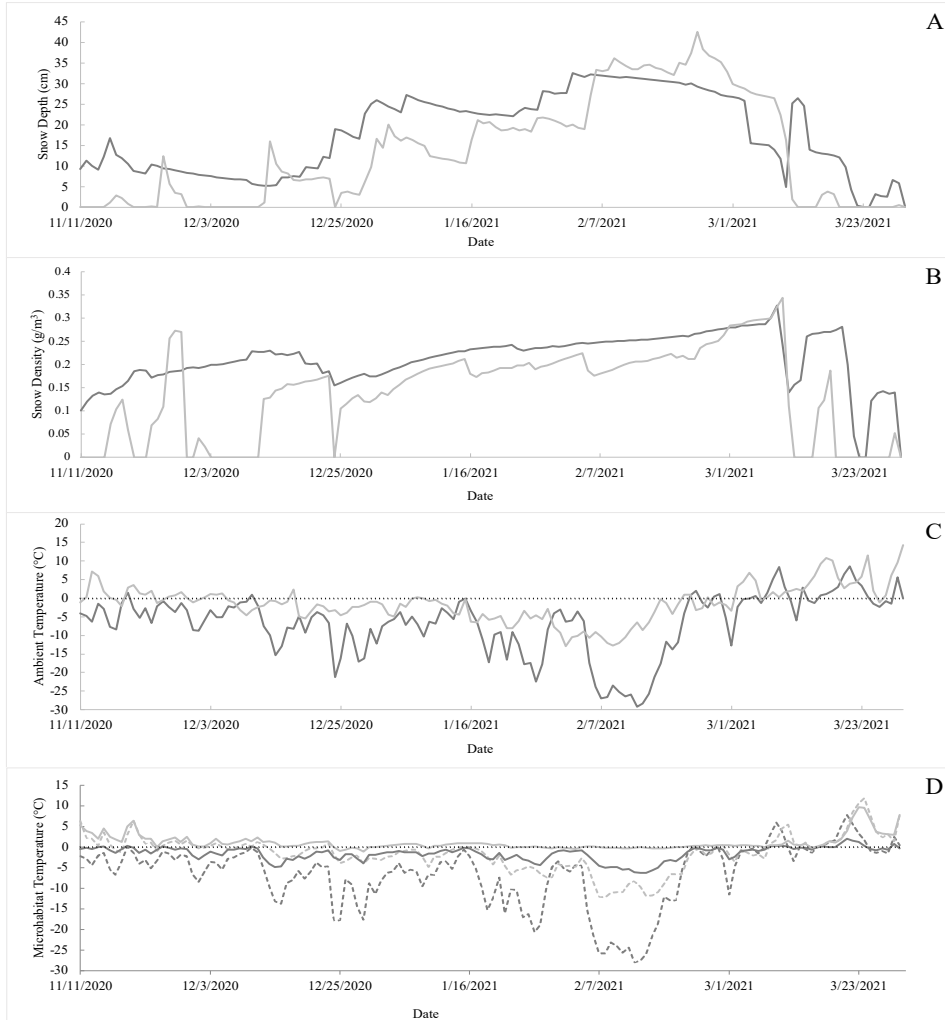


**Figure 2.3.** Daily snow depth, snow density, ambient temperature, and microsite temperature. Solid gray lines represent average daily estimates of snow conditions (a,b), ambient temperature (c), and subnivium temperatures (d) gathered in the Superior National Forest, Minnesota USA. Solid light gray lines represent empirical estimates of snow conditions (a,b), ambient temperature (c), and subnivium temperatures (d) gathered in the Manistee National Forest, Michigan USA. Dashed lines represent average daily tree cavity temperatures in the Superior National Forest (dark gray; d), and the Manistee National Forest (light gray; d).



**Figure 2.4.** Winter temperatures in tree cavities and subnivean sites in the Superior National Forest, Minnesota USA, and in the Manistee National Forest, Michigan USA. Bars represent the average monthly microsite temperature in 2020-2021. Error bars represent the 95% confidence intervals.

**Table 2.1.** Summary of tree cavity characteristics in the Superior National Forest, MN, USA, and the Manistee National Forest, MI, USA.

Cavity Characteristic	Superior National Forest, MN USA				Manistee National Forest, MI USA			
	Mean	SD	Min	Max	Mean	SD	Min	Max
Cavity volume (m <sup>3</sup> )	0.3	0.4	0.1	1.8	0.4	0.4	0.1	1.4
Wood thickness (cm)	11.2	4.4	6.0	20.7	12.1	3.9	5.1	19.8
Cavity surface area (m <sup>2</sup> )	2.8	2.5	1.0	12.2	2.9	2.0	0.8	7.7
Cavity height (cm)	188.4	125.1	61.0	591.2	137.6	70.6	41.9	289.6
Cavity diameter (cm)	41.5	11.6	26.7	64.3	54.1	18.6	26.7	105.4
Entrance hole area (cm <sup>2</sup> )	95.9	84.2	21.5	339.3	84.2	70.9	25.3	258.9

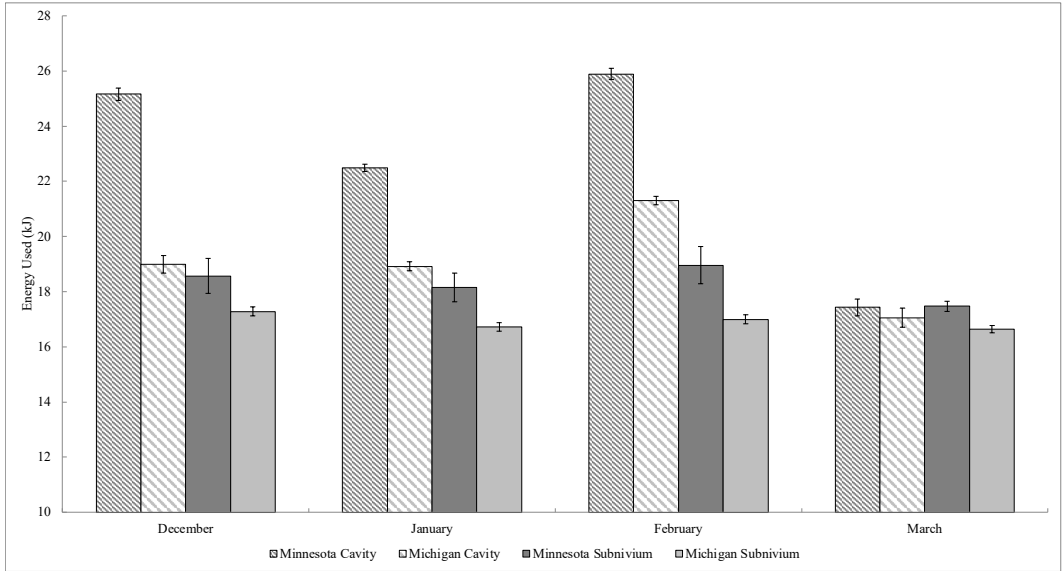


**Figure 2.5.** Energy lost while inactive for one hour in tree cavities and subnivean sites during the winter in the Superior National Forest, Minnesota USA, and in the Manistee National Forest, Michigan USA. Bars represent the average energy lost by a female across each sampled month in 2020-2021. Error bars represent the 95% confidence intervals.

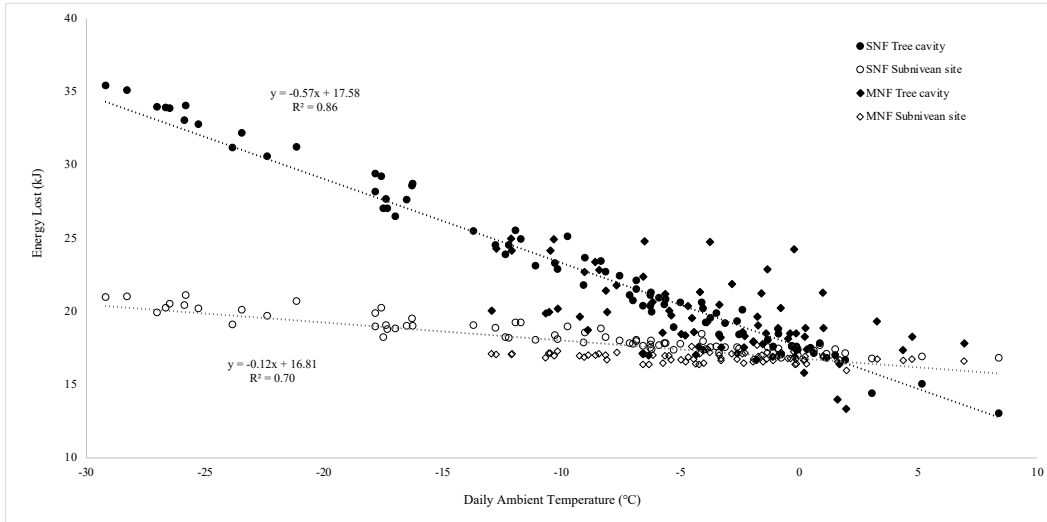


**Figure 2.6.** Relationship between ambient temperature and average energy lost while inactive for one hour a day in tree cavities (solid), and in subnivean microsites (open). Each point represents average energy lost by a female marten in the Superior National Forest, Minnesota USA (circles), and Manistee National Forest, Michigan USA (diamonds) during the winter from 2020-2021.

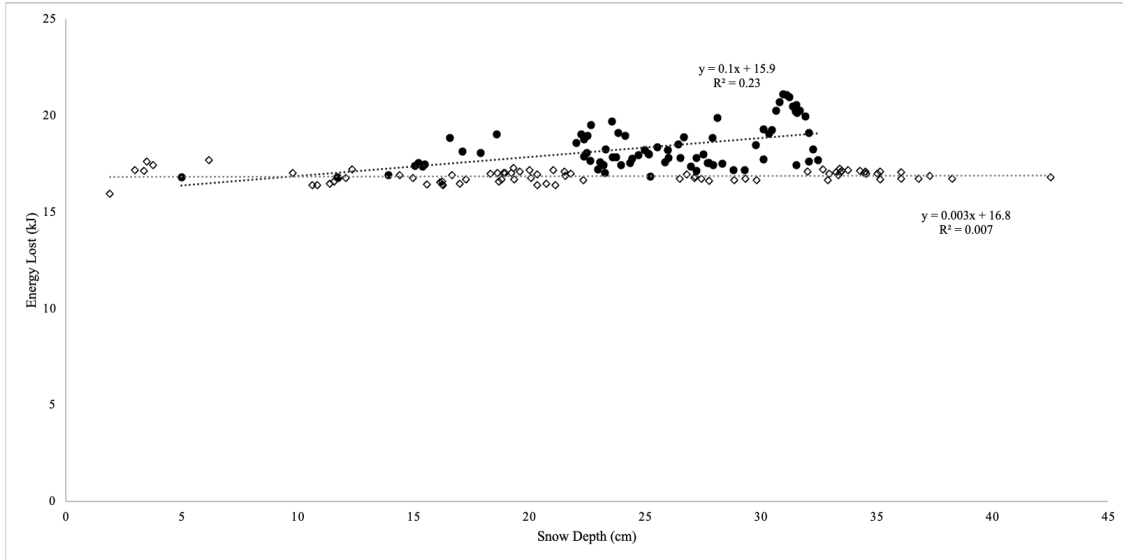


**Figure 2.7.** Relationship between snow depth and average energy lost while inactive for one hour a day in subnivean microsites. Each point represents average energy lost by a female marten in the Superior National Forest, Minnesota USA (solid circles), and Manistee National Forest, Michigan USA (empty diamonds) during winter 2020-2021.

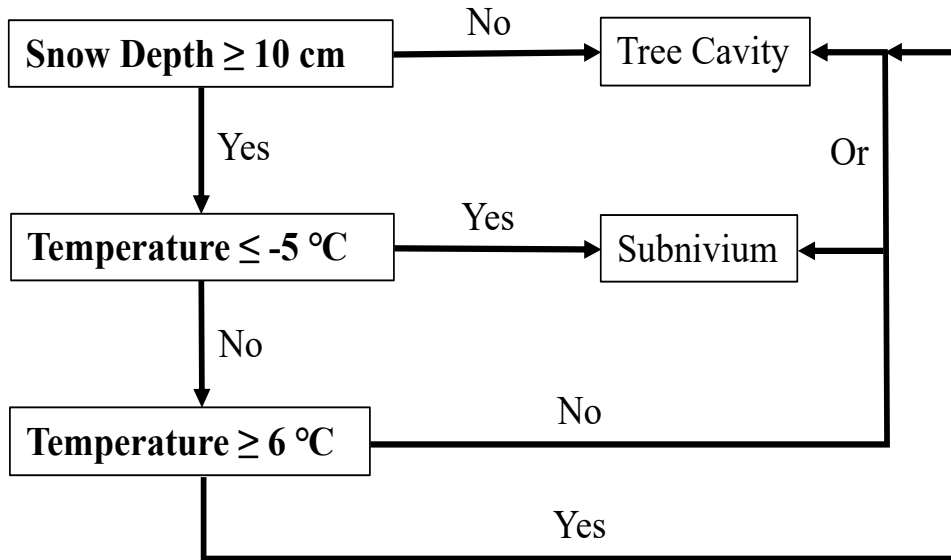


**Figure 2.8.** Modified decision tree for selecting subnivean and tree cavity microsites.

Decisions are based on snow depth and ambient temperature. Modified from Taylor and Buskirk (1994).

## Bibliography

- Al-Ajlan, S.A., 2006. Measurements of thermal properties of insulation materials by using transient plane source technique. *Appl. Therm. Eng.* 26, 2184–2191. <https://doi.org/10.1016/j.applthermaleng.2006.04.006>
- American Society of Heating, Refrigerating and Air Conditioning Engineers, 2010. ASHRAE Standard Thermal Environmental Conditions for Human Occupancy. The Society.
- Ardia, D.R., Pérez, J.H., Clotfelter, E.D., 2006. Nest box orientation affects internal temperature and nest site selection by Tree Swallows. *J. F. Ornithol.* 77, 339–344. <https://doi.org/10.1111/j.1557-9263.2006.00064.x>
- Asdrubali, F., D’Alessandro, F., Schiavoni, S., 2015. A review of unconventional sustainable building insulation materials. *Sustain. Mater. Technol.* 4, 1–17. <https://doi.org/10.1016/j.susmat.2015.05.002>
- Aubry, K.B., Raley, C.M., Buskirk, S.W., Zielinski, W.J., Schwartz, M.K., Golightly, R.T., Purcell, K.L., Weir, R.D., Yaeger, J.S., 2013. Meta-analyses of habitat selection by fishers at resting sites in the pacific coastal region. *J. Wildl. Manage.* 77, 965–974. <https://doi.org/10.1002/jwmg.563>
- Beever, E.A., Hall, L.E., Varner, J., Loosen, A.E., Dunham, J.B., Gahl, M.K., Smith, F.A., Lawler, J.J., 2017. Behavioral flexibility as a mechanism for coping with climate change. *Front. Ecol. Environ.* <https://doi.org/10.1002/fee.1502>
- Bergman, T.L., Incropera, F.P., Lavine, A.S., Dewitt, D.P., 2011. Introduction to heat transfer. John Wiley Sons.
- Berry, R., Livesley, S., Aye, L., 2013. Tree canopy shade impacts on solar irradiance received by building walls and their surface temperature. *Build. Environ.* 69, 91–100.
- Bolstad, P. V., Bentz, B.J., Logan, J.A., 1997. Modelling micro-habitat temperature for *Dendroctonus ponderosae* (Coleoptera: Scolytidae). *Ecol. Modell.* 94, 287–297. [https://doi.org/10.1016/S0304-3800\(96\)00021-X](https://doi.org/10.1016/S0304-3800(96)00021-X)
- Bryant, S.R., Shreeve, T.G., 2002. The use of artificial neural networks in ecological analysis: Estimating microhabitat temperature. *Ecol. Entomol.* 27, 424–432. <https://doi.org/10.1046/j.1365-2311.2002.00422.x>
- Bull, E.L., Heater, T.W., 2000. Resting and denning sites of American martens in Northeastern Oregon. *Northwest Sci.* 74, 179–185.

- Buskirk, S.W., 1984. Seasonal Use of Resting Sites by Marten in South-Central Alaska. *J. Wildl. Manage.* 48, 950–953.
- Buskirk, S.W., Forrest, S.C., Raphael, M.G., Harlow, H.J., 1989. Winter Resting Site Ecology of Marten in the Central Rocky Mountains. *J. Wildl. Manage.* 53, 191–196.
- Buskirk, S.W., Harlow, H.J., 1989. Body-Fat Dynamics of the American Marten (*Martes americana*) in Winter. *J. Mammal.* 70, 191–193.
- Buskirk, S.W., Harlow, H.J., Forrest, S.C., 1988. Temperature regulation in American marten in winter. *Natl. Geogr. Res.* 4, 208–214.
- Buskirk, S.W., Ruggiero, L.F., 1994. American marten, in: *The Scientific Basis for Conserving Forest Carnivores: American Marten, Fisher, Lynx, and Wolverine in the Western United States.* pp. 7–37.
- Charrier, G., Nolf, M., Leitinger, G., Charra-Vaskou, K., Losso, A., Tappeiner, U., Améglio, T., Mayr, S., 2017. Monitoring of freezing dynamics in trees: A simple phase shift causes complexity. *Plant Physiol.* 173, 2196–2207.  
<https://doi.org/10.1104/pp.16.01815>
- Clement, M.J., Castleberry, S.B., 2013. Tree structure and cavity microclimate: Implications for bats and birds. *Int. J. Biometeorol.* 57, 437–450.  
<https://doi.org/10.1007/s00484-012-0569-z>
- Cockle, K.L., Martin, K., Robledo, G., 2012. Linking fungi, trees, and hole-using birds in a Neotropical tree-cavity network: Pathways of cavity production and implications for conservation. *For. Ecol. Manage.* 264, 210–219.  
<https://doi.org/10.1016/j.foreco.2011.10.015>
- Cohen, J., 1994. Snow cover and climate. *Weather* 49, 150–156.  
<https://doi.org/10.1002/j.1477-8696.1994.tb05997.x>
- Coombs, A.B., Bowman, J., Garroway, C.J., 2010. Thermal Properties of Tree Cavities During Winter in a Northern Hardwood Forest. *J. Wildl. Manage.* 74, 1875–1881. <https://doi.org/10.2193/2009-560>
- Corn, J.G., Raphael, M.G., 1992. Habitat Characteristics at Marten Subnivean Access Sites. *J. Wildl. Manage.* 442–448.
- Croose, E., Birks, J.D.S., Martin, J., 2016. Den boxes as a tool for pine marten *Martes martes* conservation and population monitoring in a commercial forest in Scotland. *Conserv. Evid.* 13, 57–61.

- Cui, B., Fan, C., Munk, J., Mao, N., Xiao, F., Dong, J., Kuruganti, T., 2019. A hybrid building thermal modeling approach for predicting temperatures in typical, detached, two-story houses. *Appl. Energy* 236, 101–116. <https://doi.org/10.1016/j.apenergy.2018.11.077>
- Davis, L.R., Horley, S., 2015. Fisher (*Pekania pennanti*) artificial reproductive den box study. Williams Lake, British Columbia, Canada.
- De Frenne, P., Zellweger, F., Rodríguez-Sánchez, F., Scheffers, B.R., Hylander, K., Luoto, M., Vellend, M., Verheyen, K., Lenoir, J., 2019. Global buffering of temperatures under forest canopies. *Nat. Ecol. Evol.* 3, 744–749. <https://doi.org/10.1038/s41559-019-0842-1>
- Delheimer, M.S., Slauson, K.M., Szykman Gunther, M., Zielinski, W.J., 2018. Use of artificial cavities by Humboldt marten. *Wildl. Soc. Bull.* 42, 510–517. <https://doi.org/10.1002/wsb.900>
- Derby, R.W., Gates, D.M., 1966. The temperature of tree trunks-calculated and observed. *Am. J. Bot.* 53, 580–587.
- Du Plessis, M.A., Weathers, W.W., Koenig, W.D., 1994. Energetic benefits of communal roosting by acorn woodpeckers during the nonbreeding season. *Condor* 96, 631–637.
- Dunlap, F., 1912. The specific heat of wood. US Dep. Agric. For. Serv. 110.
- Dye, D.G., 2002. Variability and trends in the annual snow-cover cycle in Northern Hemisphere land areas, 1972-2000. *Hydrol. Process.* 16, 3065–3077. <https://doi.org/10.1002/hyp.1089>
- Erb, J., Coy, P., Sampson, B., 2015. Reproductive ecology of fisher and marten in Minnesota.
- Fan, Z., Shifley, S.R., Spetich, M.A., Thompson III, F.R., Larsen, D.R., 2003. Distribution of cavity trees in midwestern old-growth and second-growth forests. *Can. J. For. Res.* 33, 1481–1494.
- Fan, Z., Shifley, S.R., Spetich, M.A., Thompson III, F.R., Larsen, D.R., 2005. Abundance and Size Distribution of Cavity Trees in Second-Growth and Old-Growth Central Hardwood Forests. *North. J. Appl. For.* 22, 162–169.
- Fawcett, S., Sistla, S., Dacosta-Calheiros, M., Kahraman, A., Reznicek, A.A., Rosenberg, R., von Wettberg, E.J.B., 2019. Tracking microhabitat temperature variation with iButton data loggers. *Appl. Plant Sci.* 7, 1–12. <https://doi.org/10.1002/aps3.1237>

- Fitzpatrick, M.J., Zuckerberg, B., Pauli, J.N., Kearney, M.R., Thompson, K.L., Werner, L.C., Porter, W.P., 2019. Modeling the distribution of niche space and risk for a freeze-tolerant Ectotherm, *Lithobates Sylvaticus*. *Ecosphere* 10. <https://doi.org/10.1002/ecs2.2788>
- Flaherty, E.A., Ben-David, M., Pauli, J.N., 2014. A comparison of locomotor performance of the semiarboreal Pacific marten (*Martes caurina*) and semiaquatic mustelids. *Can. J. Zool.* 92, 259–266. <https://doi.org/10.1139/cjz-2013-0150>
- Florides, G., Kalogirou, S., 2005. Annual ground temperature measurements at various depths.
- Fountain, A.G., Campbell, J.L., Schuur, E.A.G., Stammerjohn, S.E., Williams, M.W., Ducklow, H.W., 2012. The disappearing cryosphere: Impacts and ecosystem responses to rapid cryosphere loss. *Bioscience* 62, 405–415. <https://doi.org/10.1525/bio.2012.62.4.11>
- Ge, Y., Gong, G., 2010. Land surface insulation response to snow depth variability. *J. Geophys. Res. Atmos.* 115. <https://doi.org/10.1029/2009JD012798>
- Gilad-Bachrach, R., Navot, A., Tishby, N., 2003. An information theoretic tradeoff between complexity and accuracy, in: *Lecture Notes in Computer Science*. pp. 595–609.
- Gilbert, J., Wright, J., Lauten, D., Probst, J., 1997. Den and rest-site characteristics of American marten and fisher in northern Wisconsin. *Martes Taxon. Ecol. Tech. Manag. Prov. Museum Alberta, Edmonton, Alberta, Canada* 135–145.
- Gilbert, J.H., Zollner, P.A., Green, A.K., Wright, J.L., Karasov, W.H., 2009. Seasonal field metabolic rates of american martens in Wisconsin. *Am. Midl. Nat.* 162, 327–334. <https://doi.org/10.1674/0003-0031-162.2.327>
- Graf, I., Ceseri, M., Stockie, J.M., 2015. Multiscale model of a freeze-thaw process for tree sap exudation. *J. R. Soc. Interface* 12. <https://doi.org/10.1098/rsif.2015.0665>
- Graves, A.T., Fajvan, M., Ann, J., Miller, G.W., 2000. The effects of thinning intensity on snag and cavity tree abundance in an Appalachian hardwood stand, *Canadian Journal of Forest Research*.
- Green, J.M., 2013. *Climate Change and Metapopulation Implications for Species Re/introductions: A Spatial Analysis of Suitable Habitat for the American Marten (Martes americana) in Northern Michigan*. Grand Valley State University.
- Groisman, P.Y., Knight, R.W., Karl, T.R., Easterling, D.R., Sun, B., Lawrimore, J.H., 2004. Contemporary Changes of the Hydrological Cycle over the Contiguous

- United States: Trends Derived from In Situ Observations. *J. Hydrometeorol.* 5, 64–85.
- Grüebler, M.U., Widmer, S., Korner-Nievergelt, F., Naef-Daenzer, B., 2014. Temperature characteristics of winter roost-sites for birds and mammals: Tree cavities and anthropogenic alternatives. *Int. J. Biometeorol.* 58, 629–637. <https://doi.org/10.1007/s00484-013-0643-1>
- Guiden, P.W., Connolly, B.M., Orrock, J.L., 2019. Seedling responses to decreased snow depend on canopy composition and small-mammal herbivore presence. *Ecography (Cop.)*. 42, 780–790. <https://doi.org/10.1111/ecog.03948>
- Guiden, P.W., Orrock, J.L., 2021. Snow depth and woody debris drive variation in small-mammal winter seed removal. *J. Veg. Sci.* 32. <https://doi.org/10.1111/jvs.13007>
- Halekoh, U., Højsgaard, S., Yan, J., 2006. The R Package geepack for Generalized Estimating Equations. *J. Stat. Softw.* 15/2, 1–11.
- Harlow, H., 1994. Trade-offs associated with the size and shape of American martens. *Martens, sables Fish. Biol. Conserv.* 391–403.
- Hayhoe, K., VanDorn, J., Croley, T., Schlegal, N., Wuebbles, D., 2010. Regional climate change projections for Chicago and the US Great Lakes. *J. Great Lakes Res.* 36, 7-21. <https://doi.org/10.1016/j.jglr.2010.03.012>
- Hedlund, H., Johansson, P., 2000. Heat capacity of birch determined by calorimetry: implications for the state of water in plants. *Thermochim. Acta* 349, 79–88.
- Herreid II, C.F., Kessel, B., 1967. Thermal conductance in birds and mammals. *Comp. Biochem. Physiol.* 21, 405–414.
- Hietaharju, P., Ruusunen, M., Leivisk, K., 2018. A dynamic model for indoor temperature prediction in buildings. *Energies* 11. <https://doi.org/10.3390/en11061477>
- Hudson, G., Underwood, C.P., 1999. A simple building modelling procedure for MATLAB/SIMULINK. *SIMULINK1999*.
- International Standard, 2005. ISO Standard Ergonomics of the thermal environment - Analytical determination and interpretation of thermal comfort using calculation of the PMV and PPD indices and local thermal comfort criteria. Geneva, Switzerland: International Standards Organization
- Isaac, J.L., De Gabriel, J.L., Goodman, B.A., 2008. Microclimate of daytime den sites in a tropical possum: Implications for the conservation of tropical arboreal

marsupials. *Anim. Conserv.* 11, 281–287. <https://doi.org/10.1111/j.1469-1795.2008.00177.x>

Joyce, M.J., 2013. Space use behavior and multi-scale habitat selection of American marten (*Martes americana*) in northeastern Minnesota.

Joyce, M.J., Zalewski, A., Erb, J.D., Moen, R.A., 2017. Use of resting microsites by members of the *Martes* complex: the role of thermal stress across species and regions, in: *The Martes Complex in the 21st Century: Ecology and Conservation*. pp. 181–221.

Jylhä, K., Fronzek, S., Tuomenvirta, H., Carter, T.R., Ruosteenoja, K., 2008. Changes in frost, snow and Baltic sea ice by the end of the twenty-first century based on climate model projections for Europe. *Clim. Change* 86, 441–462. <https://doi.org/10.1007/s10584-007-9310-z>

Kamke, F.A., 1989. Thermal Conductivity of Wood-Based Panels, in: Hasselman, D.P.H., Thomas, J.R. (Eds.), *Thermal Conductivity* 20. Springer US, Boston, MA, pp. 249–259. [https://doi.org/10.1007/978-1-4613-0761-7\\_24](https://doi.org/10.1007/978-1-4613-0761-7_24)

Kausrud, K.L., Mysterud, A., Steen, H., Vik, J.O., Østbye, E., Cazelles, B., Framstad, E., Eikeset, A.M., Mysterud, I., Solhøy, T., Stenseth, N.C., 2008. Linking climate change to lemming cycles. *Nature* 456, 93–97. <https://doi.org/10.1038/nature07442>

Kearney, M.R., 2020. How will snow alter exposure of organisms to cold stress under climate warming? *Glob. Ecol. Biogeogr.* 29, 1246–1256. <https://doi.org/10.1111/geb.13100>

Kearney, M.R., Porter, W.P., 2017. NicheMapR – an R package for biophysical modelling: the microclimate model. *Ecography (Cop.)*. 40, 664–674. <https://doi.org/10.1111/ecog.02360>

Kearney, M.R., Shamakhy, A., Tingley, R., Karoly, D.J., Hoffmann, A.A., Briggs, P.R., Porter, W.P., 2014. Microclimate modelling at macro scales: A test of a general microclimate model integrated with gridded continental-scale soil and weather data. *Methods Ecol. Evol.* 5, 273–286. <https://doi.org/10.1111/2041-210X.12148>

Kendeigh, C., 1961. Energy of birds conserved by roosting in cavities. *Wilson Bull.* 73, 140–147.

Kenefic, L.S., Nyland, R.D., 2007. Cavity Trees, Snags, and Selection Cutting: A Northern Hardwood Case Study. *North. J. Appl. For.* 24, 192–196.

- Kossak, B., Stadler, M., 2015. Adaptive thermal zone modeling including the storage mass of the building zone. *Energy Build.* 109, 407–417. <https://doi.org/https://doi.org/10.1016/j.enbuild.2015.10.016>
- Kudriavtcev, S., Paramonov, V., Sakharov, I., 2016. Strengthening Thawed Permafrost Base Railway Embankments Cutting Berms. *MATEC Web Conf.* 73. <https://doi.org/10.1051/mateconf/20167305002>
- Lammertink, M., Fernández, J.M., Cockle, K.L., 2019. Helmeted Woodpeckers roost in decay-formed cavities in large living trees: A clue to an old-growth forest association. *Condor Ornithol. Appl.* 121. <https://doi.org/10.1093/condor/duy016>
- Lausen, C.L., Barclay, R.M.R., 2003. Thermoregulation and roost selection by reproductive female big brown bats (*Eptesicus fuscus*) roosting in rock crevices. *J. Zool.* 260, 235–244. <https://doi.org/10.1017/S0952836903003686>
- Leuzinger, S., Vogt, R., Körner, C., 2010. Tree surface temperature in an urban environment. *Agric. For. Meteorol.* 150, 56–62. <https://doi.org/10.1016/j.agrformet.2009.08.006>
- Lindenmayer, D.B., Blanchard, W., McBurney, L., Blair, D., Banks, S., Likens, G.E., Franklin, J.F., Laurance, W.F., Stein, J.A.R., Gibbons, P., 2012. Interacting Factors Driving a Major Loss of Large Trees with Cavities in a Forest Ecosystem. *PLoS One* 7. <https://doi.org/10.1371/journal.pone.0041864>
- Lintunen, A., Hölttä, T., Kulmala, M., 2013. Anatomical regulation of ice nucleation and cavitation helps trees to survive freezing and drought stress. *Sci. Rep.* 3, 1–7. <https://doi.org/10.1038/srep02031>
- Maclean, I.M.D., Suggitt, A.J., Wilson, R.J., Duffy, J.P., Bennie, J.J., 2017. Fine-scale climate change: modelling spatial variation in biologically meaningful rates of warming. *Glob. Chang. Biol.* 23, 256–268. <https://doi.org/10.1111/gcb.13343>
- MacLean, J., 1941. Thermal conductivity of wood. *Heating, piping, air Cond.* 13, 380–391.
- Marchand, P.J., 2014. *Life in the cold: an introduction to winter ecology.* UPNE.
- Martin, M.E., Moriarty, K.M., Pauli, J.N., 2020. Forest structure and snow depth alter the movement patterns and subsequent expenditures of a forest carnivore, the Pacific marten. *Oikos* 129, 356–366. <https://doi.org/10.1111/oik.06513>
- Martin, M.E., Moriarty, K.M., Pauli, J.N., 2021. Landscape seasonality influences the resource selection of a snow-adapted forest carnivore, the Pacific marten. *Landsc. Ecol.* 36, 1055–1069. <https://doi.org/10.1007/s10980-021-012159>

- Martin, S.K., 1987. The ecology of the pine marten (*Martes americana*) at Sagehen Creek, California. University of California, Berkeley.
- Matthews, S.M., Green, D.S., Higley, J.M., Rennie, K.M., Kelsey, C.M., Green, R.E., 2019. Reproductive den selection and its consequences for fisher neonates, a cavity-obligate mustelid. *J. Mammal.* 100, 1305–1316. <https://doi.org/10.1093/jmammal/gyz069>
- Maziarz, M., Broughton, R.K., Wesolowski, T., 2017. Microclimate in tree cavities and nest-boxes: Implications for hole-nesting birds. *For. Ecol. Manage.* 389, 306–313. <https://doi.org/10.1016/j.foreco.2017.01.001>
- McCann, N.P., Zollner, P.A., Gilbert, J.H., 2017. Temporal scaling in analysis of animal activity. *Ecography (Cop.)*. 40, 1436–1444. <https://doi.org/10.1111/ecog.02742>
- McComb, W.C, Noble, R.E, 1981. Microclimates of nest boxes and natural cavities in bottomland hardwoods. *J. Wildl. Manage.* 45, 284–289.
- McComb, W.C., Noble, R.E., 1981. Herpetofaunal use of natural tree cavities and nest boxes. *Wildl. Soc. Bull.* 261–267.
- Méndez-Toribio, M., Meave, J.A., Zermeño-Hernández, I., Ibarra-Manríquez, G., 2016. Effects of slope aspect and topographic position on environmental variables, disturbance regime and tree community attributes in a seasonal tropical dry forest. *J. Veg. Sci.* 27, 1094–1103. <https://doi.org/10.1111/jvs.12455>
- Mersten-Katz, C., Barnea, A., Yom-Tov, Y., Ar, A., 2012. The woodpecker’s cavity microenvironment: Advantageous or restricting? *Avian Biol. Res.* 5, 227–237. <https://doi.org/10.3184/174751912X13530894822224>
- Moore, A.D., 1945. Winter night habits of birds. *Wilson Bull.* 57, 253–260.
- Moritz, C., Agudo, R., 2013. The future of species under climate change: resilience or decline? *Science.* 341, 504–508.
- National Operational Hydrologic Remote Sensing Center. 2004. Snow Data Assimilation System (SNODAS) Data Products at NSIDC, Version 1. Boulder, Colorado USA. NSIDC: National Snow and Ice Data Center. <https://doi.org/10.7265/N5TB14TC>.
- Newbury, R.K., Hodges, K.E., 2019. A winter energetics model for bobcats in a deep snow environment. *J. Therm. Biol.* 80, 56–63. <https://doi.org/10.1016/j.jtherbio.2019.01.006>
- Osanyintola, O.F., Talukdar, P., Simonson, C., 2005. Experimental and Numerical Studies of Transient Heat and Moisture Transfer within Spruce Plywood 0, 1–14.

- Paclík, M., Weidinger, K., 2007. Microclimate of tree cavities during winter nights - Implications for roost site selection in birds. *Int. J. Biometeorol.* 51, 287–293. <https://doi.org/10.1007/s00484-006-0067-2>
- Pauli, J.N., Zuckerberg, B., Whiteman, J.P., Porter, W., 2013. The subnivium: A deteriorating seasonal refugium. *Front. Ecol. Environ.* 11, 260–267. <https://doi.org/10.1890/120222>
- Petty, S.K., Zuckerberg, B., Pauli, J.N., 2015. Winter conditions and land cover structure the subnivium, a seasonal refuge beneath the snow. *PLoS One* 10, 1–12. <https://doi.org/10.1371/journal.pone.0127613>
- Popiel, C.O., Wojtkowiak, J., Biernacka, B., 2001. Measurements of temperature distribution in ground. *Exp. Therm. fluid Sci.* 25, 301–309.
- Potter, B.E., Andresen, J.A., 2002. A finite-difference model of temperatures and heat flow within a tree stem. *Can. J. For. Res.* 32, 548–555. <https://doi.org/10.1139/x01-226>
- Powell, R.A., 1979. Ecological Energetics and Foraging Strategies of the Fisher (*Martes pennanti*). *J. Anim. Ecol.* 48, 195–212.
- Powell, R.A., Leonard, R.D., 1983. Sexual Dimorphism and Energy Expenditure for Reproduction in Female Fisher *Martes pennanti*. *Oikos* 40, 166–174.
- PRISM [Parameter-elevation Regressions on Independent Slopes Model] Climate Group, Oregon State University, <http://prism.oregonstate.edu>
- R Core Team. 2021. R: A language and environment for statistical computing. R Foundation for Statistical Computing, Vienna, Austria. <https://www.R-project.org/>
- Radmanović, K., Dukić, I., Pervan, S., 2014. Specific Heat Capacity of Wood. *Drv. Ind.* 65, 151–157. <https://doi.org/10.5552/drind.2014.1333>
- Ragland, K.W., Aerts, D.J., Baker, A.J., 1991. Properties of Wood for Combustion Analysis, Bioresource Technology.
- Reid, S., Driller, T., Watson, M., 2020. A two-dimensional heat transfer model for predicting freeze-thaw events in sugar maple trees. *Agric. For. Meteorol.* 294, 108139. <https://doi.org/10.1016/j.agrformet.2020.108139>
- Remm, J., Lõhmus, A., 2011. Tree cavities in forests - The broad distribution pattern of a keystone structure for biodiversity. *For. Ecol. Manage.* <https://doi.org/10.1016/j.foreco.2011.04.028>

- Repola, J., 2006. Models for Vertical Wood Density of Scots Pine, Norway Spruce and Birch Stems, and Their Application to Determine Average Wood Density. *Silva Fenn.* 40.
- Ruczyński, I., 2006. Influence of temperature on maternity roost selection by noctule bats (*Nyctalus noctula*) and Leisler's bats (*N. leisleri*) in Białowieża Primeval Forest, Poland. *Can. J. Zool.* 84, 900–907. <https://doi.org/10.1139/Z06-060>
- Ruggiero, L.F., Pearson, E., Henry, S.E., 1998. Characteristics of American Marten Den Sites in Wyoming. *J. Wildl. Manage.* 62, 663–673.
- Sanders, R.L., Cornman, A., Keenlance, P., Jacquot, J.J., Unger, D.E., Spriggs, M., 2017. Resting Site Characteristics of American Marten in the Northern Lower Peninsula of Michigan. *Am. Midl. Nat.* 177, 211–225. <https://doi.org/10.1674/0003-0031-177.2.211>
- Scheffers, B.R., Edwards, D.P., Diesmos, A., Williams, S.E., Evans, T.A., 2014. Microhabitats reduce animal's exposure to climate extremes. *Glob. Chang. Biol.* 20, 495–503. <https://doi.org/10.1111/gcb.12439>
- Scholander, P.F., 1955. Evolution of Climatic Adaptation in Homeotherms.
- Sedgely, J.A., 2001. Quality of cavity microclimate as a factor influencing selection of maternity roosts by a tree-dwelling bat, *Chalinolobus tuberculatus*, in New Zealand. *J. Appl. Ecol.* 38, 425–438. <https://doi.org/10.1046/j.1365-2664.2001.00607.x>
- Singh, V.K., Tiwari, K.N., 2017. Prediction of greenhouse micro-climate using artificial neural network. *Appl. Ecol. Environ. Res.* 15, 767–778. [https://doi.org/10.15666/aeer/1501\\_767778](https://doi.org/10.15666/aeer/1501_767778)
- Skaar, C., 2012. Wood-water relations. Springer Science & Business Media.
- Slauson, K.M., Zielinski, W.J., 2009. Characteristics of summer and fall diurnal resting habitat used by american martens in coastal northwestern California. *Northwest Sci.* 83, 35–45. <https://doi.org/10.3955/046.083.0104>
- Spencer, W.D., 1987. Seasonal Rest-Site Preferences of Pine Martens in the Northern Sierra Nevada. *J. Wildl. Manage.* 51, 616–621.
- Stocks, B.J., Fosberg, M.A., Lynham, T.J., Mearns, L., Wotton, B.M., Yang, Q., Jin, J.-Z., Lawrence, K., Hartley, G.R., Mason, J.A., Mckenney, D.W., 1998. Climate change and forest fire potential in Russian and Canadian boreal forests. *Clim. Change* 38, 1–13.

- Suggitt, A.J., Gillingham, P.K., Hill, J.K., Huntley, B., Kunin, W.E., Roy, D.B., Thomas, C.D., 2011. Habitat microclimates drive fine-scale variation in extreme temperatures. *Oikos* 120, 1–8. <https://doi.org/10.1111/j.1600-0706.2010.18270.x>
- Taylor, S.L., Buskirk, S.W., 1994. Forest microenvironments and resting energetics of the American marten *Martes americana*. *Ecography (Cop.)*. 17, 249–256.
- TenWolde, A., McNatt, J.D., Krahn, L., 1988. Thermal properties of wood and wood panel products for use in buildings. For. Serv. Madison, WI (USA). For. Prod. Lab.
- Thompson, I.D., Colgan, P.W., 1994. Marten Activity in Uncut and Logged Boreal Forests in Ontario. *J. Wildl. Manage.* 58, 280–288.
- Thompson, K.L., Zuckerberg, B., Porter, W.P., Pauli, J.N., 2018. The phenology of the subnivium. *Environ. Res. Lett.* 13. <https://doi.org/10.1088/1748-9326/aac670>
- Vonhof, M.J., Barclay, R.M., 1997. Use of tree stumps as roosts by the western long-eared bat. *J. Wildl. Manage.* 674–684.
- Westermann, S., Schuler, T. V., Gisnas, K., Etzelmüller, B., 2013. Transient thermal modeling of permafrost conditions in Southern Norway. *Cryosphere* 7, 719–739. <https://doi.org/10.5194/tc-7-719-2013>
- Wiebe, K.L., 2001. Microclimate of tree cavity nests: Is it important for reproductive success in northern flickers? *Auk* 118, 412–421. <https://doi.org/10.2307/4089802>
- Wiebe, K.L., Swift, T.L., 2001. Clutch size relative to tree cavity size in Northern Flickers. *J. Avian Biol.* 32, 167–173. <https://doi.org/10.1034/j.1600-048X.2001.320210.x>
- Wilbert, C.J., Buskirk, S.W., Gerow, K.G., 2000. Effects of weather and snow on habitat selection by American martens (*Martes americana*).
- Williams, C.M., Henry, H.A.L., Sinclair, B.J., 2015. Cold truths: How winter drives responses of terrestrial organisms to climate change. *Biol. Rev.* 90, 214–235. <https://doi.org/10.1111/brv.12105>
- Worthen, G.L., Kilgore, D.L., 1981. Metabolic Rate of Pine Marten in Relation to Air Temperature. *J. Mammal.* 62, 624–628.
- Yom-Tov, Y., Yom-Tov, S., Jarrell, G., 2008. Recent increase in body size of the American marten *Martes americana* in Alaska.

- Zalewski, A., 1997. Factors affecting selection of resting site type by pine marten in primeval deciduous forests (Białowieża National Park, Poland). *Acta Theriol. (Warsz)*. 42, 271–288. <https://doi.org/10.4098/AT.arch.97-29>
- Zalewski, A., 2000. Factors affecting the duration of activity by pine martens (*Martes martes*) in the Białowieża National Park, Poland. *J. Zool.* 251, 439–447.
- Zalewski, A., 2001. Seasonal and sexual variation in diel activity rhythms of pine marten *Martes martes* in the Białowieża National Park (Poland). *Acta Theriol. (Warsz)*. 46, 295–304.
- Zalewski, A., 2005. Geographical and seasonal variation in food habits and prey size of European pine martens, in: *Martens and Fishers (Martes) in Human-Altered Environments*. Springer, pp. 77–98.
- Zarrinderakht, M., Konrad, I., Wilmot, T.R., Perkins, T.D., Berg, A. van den, Stockie, J.M., 2021. Experimental and computational comparison of freeze-thaw induced pressure generation in red and sugar maple.
- Zeger, L., Liang, S., 1986. Longitudinal Data Analysis for Discrete and Continuous Outcomes. *Biometrics* 42, 121–130.
- Zhang, M., Zhang, X., Lai, Y., Lu, J., Wang, C., 2020. Variations of the temperatures and volumetric unfrozen water contents of fine-grained soils during a freezing–thawing process. *Acta Geotech.* 15, 595–601. <https://doi.org/10.1007/s11440-018-0720-z>
- Zhao, Yue, Tian, H., Han, Q., Gu, J., Zhao, Yandong, 2021. Real-time monitoring of water and ice content in plant stem based on latent heat changes. *Agric. For. Meteorol.* 307, 108475. <https://doi.org/10.1016/j.agrformet.2021.108475>
- Zhou, J., Wei, C., Lai, Y., Wei, H., Tian, H., 2018. Application of the Generalized Clapeyron Equation to Freezing Point Depression and Unfrozen Water Content. *Water Resour. Res.* 54, 9412–9431. <https://doi.org/10.1029/2018WR023221>
- Zhu, L., Ives, A.R., Zhang, C., Guo, Y., Radeloff, V.C., 2019. Climate change causes functionally colder winters for snow cover-dependent organisms. *Nat. Clim. Chang.* 9, 886–893. <https://doi.org/10.1038/s41558-019-0588-4>
- Zielinski, W.J., Spencer, W.D., Barrett, R.H., 1983. Relationship between food habits and activity patterns of pine martens. *J. Mammal.* 64, 387–396.
- Zuckerberg, B., Pauli, J.N., 2018. Conserving and managing the subnivium. *Conserv. Biol.* 32, 774–781. <https://doi.org/10.1111/cobi.13091>

## Appendix

### A. Energy lost while inactive model

Energy lost while inactive ( $C_i$ ) can be modeled using an approach similar to that used by previous researchers (Newbury and Hodges, 2019; Powell, 1979; Powell and Leonard, 1983). Because martens frequently rest at temperatures below their lower critical temperature ( $T_{lc}$ ) during winter (Buskirk et al., 1988), the model of  $C_i$  must include terms for energetic costs of resting and thermoregulation while resting:

$$C_i = C_r + I_t C_t$$

where  $C_r$  is the energetic cost of resting when resting temperature ( $T_r$ ) is within their thermal neutral zone,  $C_t$  is the energetic cost of thermoregulation when resting temperature is below  $T_{lc}$ , and  $I_t$  is an indicator variable. When resting at or above  $T_{lc}$ ,  $C_t$  is equal to 0.  $I_t$  is therefore defined as  $I_t = 0$  when  $T_r$  greater than or equal to  $T_{lc}$  and  $I_t = 1$  when  $T_r$  is less than  $T_{lc}$ .

#### ***Energetic cost of resting, $C_r$ :***

The energetic cost of resting in a mammal's thermal neutral zone ( $C_r$ ) can be approximated empirically using a respirometer to measure  $O_2$  consumption by resting martens at thermoneutrality. Buskirk et al. (1988) estimated oxygen consumption at thermoneutrality as  $0.508 \text{ ml } O_2 \text{ g}^{-1} \text{ hr}^{-1}$ . Assuming martens expend 4.8 cal per ml  $O_2$  consumed (Herreid & Kessel 1967), and the average weight of a female marten is 625 g and weight of a male marten is 964 g (J. Erb, unpublished data),  $C_r$  of average female and male martens in kJ/hr is:

$$C_{r,females} = 6.38t_r \quad C_{r,males} = 9.84t_r$$

#### ***Energetic cost of thermoregulation, $C_t$ :***

Herreid and Kessel (1967) provided the following formula for estimating the energetic cost of thermoregulation:

$$Q_L = C * (T_b - T_a)$$

where  $Q_L$  is the heat loss from thermoregulation (equivalent to  $C_t$  as defined above),  $C$  is thermal conductance (units:  $\text{cal g}^{-1} \text{ hr}^{-1} \text{ }^\circ\text{C}^{-1}$ ),  $T_b$  is core body temperature, and  $T_a$  is ambient temperature (analogous to the temperature of the microsite ( $T_r$ ) for a resting animal). Because the energetic cost of thermoregulation is equal to 0 when animals are at or above their  $T_{lc}$ , we modified the above expression as follows:

$$C_t = C * (T_{lc} - T_r)$$

Buskirk et al. (1988) reported a conductance value of  $0.0527 \text{ ml O}_2 \text{ g}^{-1} \text{ hr}^{-1} \text{ }^\circ\text{C}^{-1}$  for winter-acclimated martens. Converting to energy units using  $4.8 \text{ cal/ml O}_2$  consumed (Herreid II and Kessel, 1967), thermal conductance of martens was estimated to be  $0.66 \text{ kJ hr}^{-1} \text{ }^\circ\text{C}^{-1}$  for adult females ( $W = 625 \text{ g}$ ) and  $1.02 \text{ kJ hr}^{-1} \text{ }^\circ\text{C}^{-1}$  for adult males ( $W = 964 \text{ g}$ ). Therefore, the energetic cost of thermoregulation for martens resting below their  $T_{lc}$  is estimated as:

$$\text{Females: } C_t = 0.66 * (T_{lc} - T_r) * t_r$$

$$\text{Males: } C_t = 1.02 * (T_{lc} - T_r) * t_r$$

Buskirk et al. (1988) estimated  $T_{lc}$  of winter-acclimated martens as  $16^\circ\text{C}$ .

***Final model of energy lost while inactive,  $C_i$ :***

Combining the models for  $C_r$  and  $C_t$  described above, the model of energetic loss while inactive (in kJ) for a marten resting at a  $T_r$  for a known time  $t_r$  is:

$$\text{Females: } C_i = 6.38 * t_r + I_r * 0.66 * (16 - T_r) * t_r$$

$$\text{Males: } C_i = 9.84 * t_r + I_r * 1.02 * (16 - T_r) * t_r$$